PS/Int. EA 60-14
13th October 1960

MAGNETIC MEASUREMENTS ON THE BENDING MAGNETS OF THE BEAM TRANSPORT SYSTEM OF THE CERN P.S.

1. GENERAL DESCRIPTION.

For the deflection of charged particle beams from the CERN P.S. a number of bending magnets have been constructed. Their pole faces are plane and rectangular. Most of the magnets have straight poles. To obtain a somewhat higher flux density over a narrower width some of the magnets have tapered poles. A cross-section of the magnets is shown in Fig. 1. The axial length of the poles is 1 metre for some of the magnets and 2 metres for the remaining ones. In terms of pole profile and length there are thus four different types. The nominal distance between the pole faces is 0.14 metre. It can be changed, however, to 0.11 m, 0.17 m or 0.20 m, by changing the spacing plates indicated by the dimension H in Fig. 1. The coils have hollow water cooled conductors. The nominal resistance is 0.2 ohm for all magnets.

The magnets are mounted on concrete supporting blocks. The blocks which also may act as radiation shielding are fitted with special devices for fine adjustment of position and orientation of the magnets.

The main parameters are collected in Table 1.

2. METHODS OF MEASUREMENT.

2.1. Definitions and symbols.

The coordinate system used is indicated in Fig. 1. Some definitions and symbols are given below.

B_{zo} = Flux density in z-direction at the point (0,0,0)

I_M = Magnet excitation current

$L_{eq} = \frac{1}{B_{zo}} \int_{-\infty}^{+\infty} B_z(y)\, dy$ = Equivalent length

$P = \int_{-\infty}^{+\infty} B_z(y)\, dy$ = Bending power

2.2. The magnetisation curve.

The magnetisation curve $B_{zo}(I_M)$ was measured by means of the Hall effect. The circuit used is indicated schematically in Fig. 2. The Hall voltage and the Hall current were both measured by means of a compensator.

2.3. Distribution of the flux density.

The transverse distribution (in x - direction) of

$$\frac{B_{z,x} - B_{z,o}}{B_{,z,o}} = \frac{\Delta B}{B}$$

was measured by means of the Hall effect. The signal from a moveable Hall plate was opposed to the signal from a fixed reference Hall plate. The difference signal from the two matched Hall plates was measured with a millivolt-meter of high internal resistance, when necessary after some electronic amplification. By this difference method the influence of fluctuations in magnet current is practically eliminated.

2.4. Bending power and equivalent length.

The bending power

$$P = \int_{-\infty}^{+\infty} B_z(y)\, dy$$

was first determined well below saturation (at 0.64 Wb/m^2) by means of graphical integration of Hall effect point measurements. The same quantity was then measured by means of a long narrow coil and an electronic integrator. The length of the coil was 4 m and its width 20 mm. The effective area was of the order of 1 m^2.

These two measurements provide a direct conversion constant

$$K = \frac{\int_{-\infty}^{+\infty} B_z(y)\, dy}{V_i}$$

for conversion from integrator voltage V_i to magnetic bending power. The bending power as a function of current was then measured with the long coil and the integrator.

The transverse distribution was determined by transverse displacement of the coil between the position $x = a$ and $x = o$.

The integrator output voltage is then directly proportional to the difference in bending power at $x = a$ and $x = o$. In this way the effect of drift in the measuring apparatus and the magnet current is reduced to a minimum.

The equivalent length

$$L_{eq} = \frac{1}{B_{z,o}} \int_{-\infty}^{+\infty} B_z(y)\, dy$$

is obtained by simple calculation of the ratio between bending power and flux density.

2.5. Correction for saturation and edge effect.

A uniform distribution of B and P over a rectangular area was aimed at. This was approached by mounting shims on the pole faces (Fig. 1) and end pieces on the ends of the poles. The distribution of B and P was measured at various values of flux density for different combinations of shims and end pieces.

From the resulting curves it should be easy to select the most suitable shim to achieve an optimum of the distribution of B and P for any given value of P.

3. RESULTS AND CONCLUSION.

The flux density and bending power as a function of magnet current are given in Fig. 3 and Fig. 4 for all four magnet types. The transverse distributions of the same quantities are given in Fig. 5 - Fig. 16. The best distribution of B for magnets fitted with standard (7 x 30 mm^2) shims (see Fig. 1) occurs at about 1.1 Wb/m^2 for the magnets with straight poles and at about 1.4 Wb/m^2 for magnets with tapered poles. The optimum distribution of P at the same values of B are obtained by fitting end pieces of dimensions (12 x 130 + 12 x 80) mm^2 and 20 x 130 mm^2 for the straight and tapered pole profiles respectively (see Fig. 1) With standard shims but no end pieces the optimum distributions of P occur at 0.5 Wb/m^2 and 1.0 Wb/m^2 respectively.

A comparison of the characteristics Fig. 5 - Fig. 16 indicates a close resemblance between the transverse distributions of both B and P for the 1 metre and the 2 metre magnets of same pole profile. More detailed characteristics are therefore given only for the 1 metre magnets. Fig. 17 - Fig. 30 show the effect of different shim thickness on the distribution of flux density and bending power for the two different types of 1 metre magnets.

B. Langeseth
G. Pluym
B. de Raad

/fv

Distribution : (open)
PBC Group
Parameter Committee

T A B L E 1

Type	1 metre Bending Magnet Straight Poles	2 metre Bending Magnet Straight Poles	1 metre Bending Magnet Tapered Poles	2 metre Bending Magnet Tapered Poles
Pole face	1 m x 0.52 m	2 m x 0.52 m	1 m x 0.42 m	2 m x 0.42 m
Gap height	for all types 0.11 , 0.14 nominal, 0.17 and 0.20 m			
Nominal Current I_N	675 A	830 A	675 A	830 A
Bending power at I_N	1.88 Wb/m	3.63 Wb/m	1.96 Wb/m	3.80 Wb/m
Flux density at I_N	1.64 Wb/m^2	1.74 Wb/m^2	1.74 Wb/m^2	1.84 Wb/m^2
Resistance at 20°C	for all types 0.195 ohm			
Max. temp.	for all types 40° C at inlet and 80° C at outlet			
Weight of magnet and base	15 + 3 ton	30 + 6 ton	15 + 3 ton	30 + 6 ton

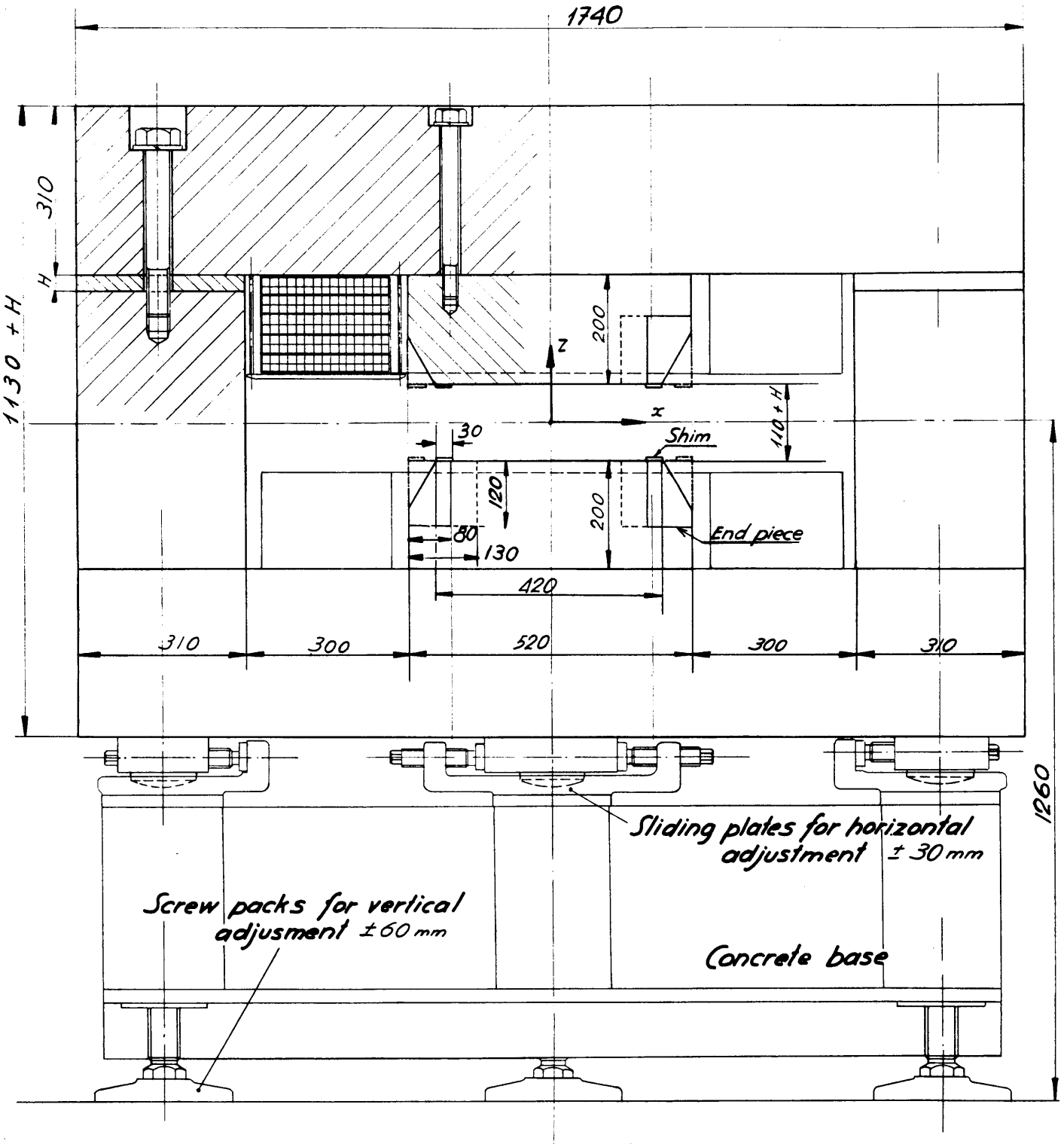

H: 0 ; 30 mm (nominal) ; 60 mm or 90 mm.
Adjustable by spacing plates

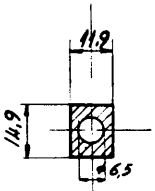

Conductor for 1 meter magnet
180 turns per pole

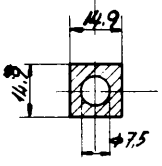

Conductor for 2 meter magnet
150 turns per pole

Fig. 1 Cross-section of bending magnets

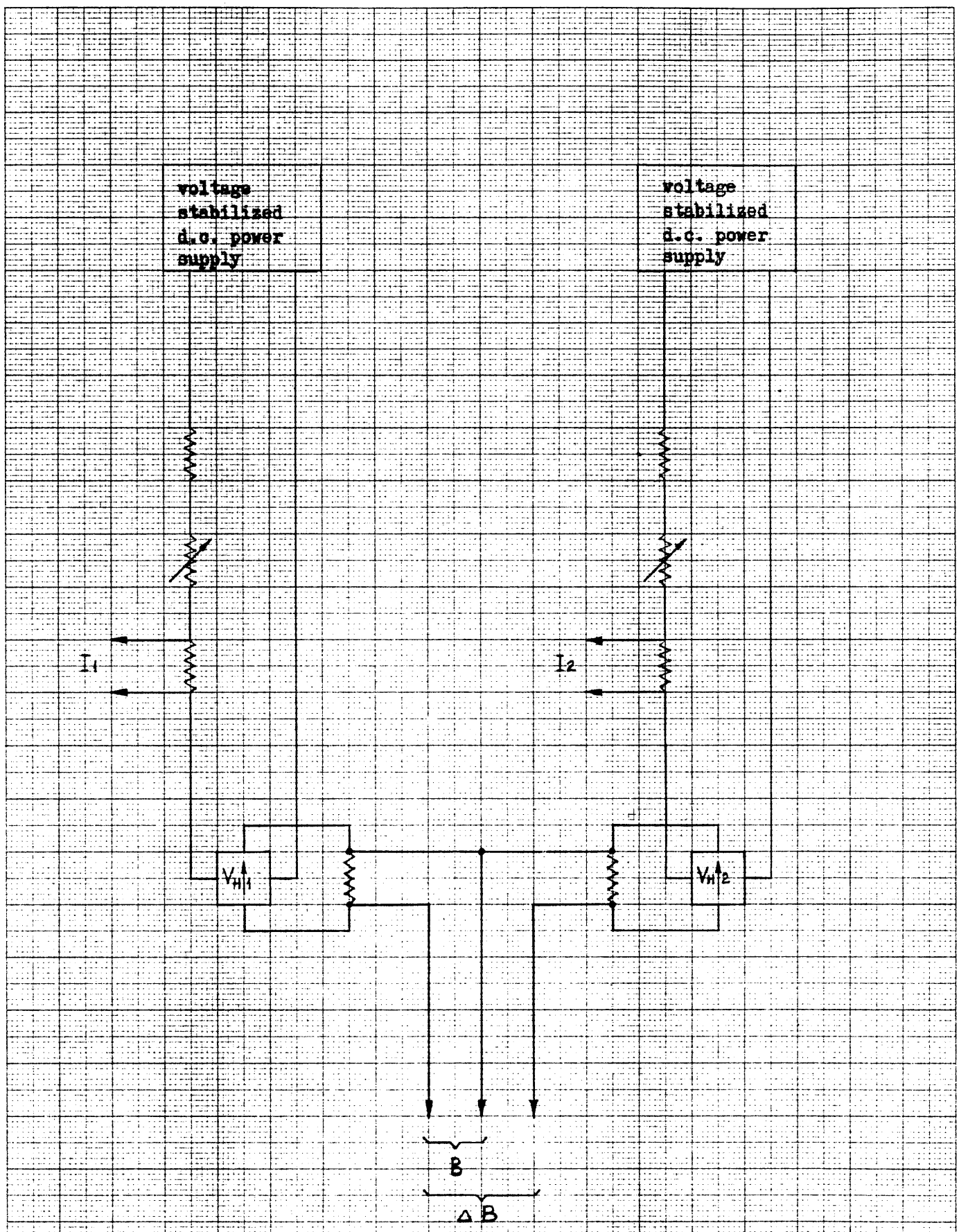

Fig. 2 Hall Generator Circuit for Magnetic Field Measurements

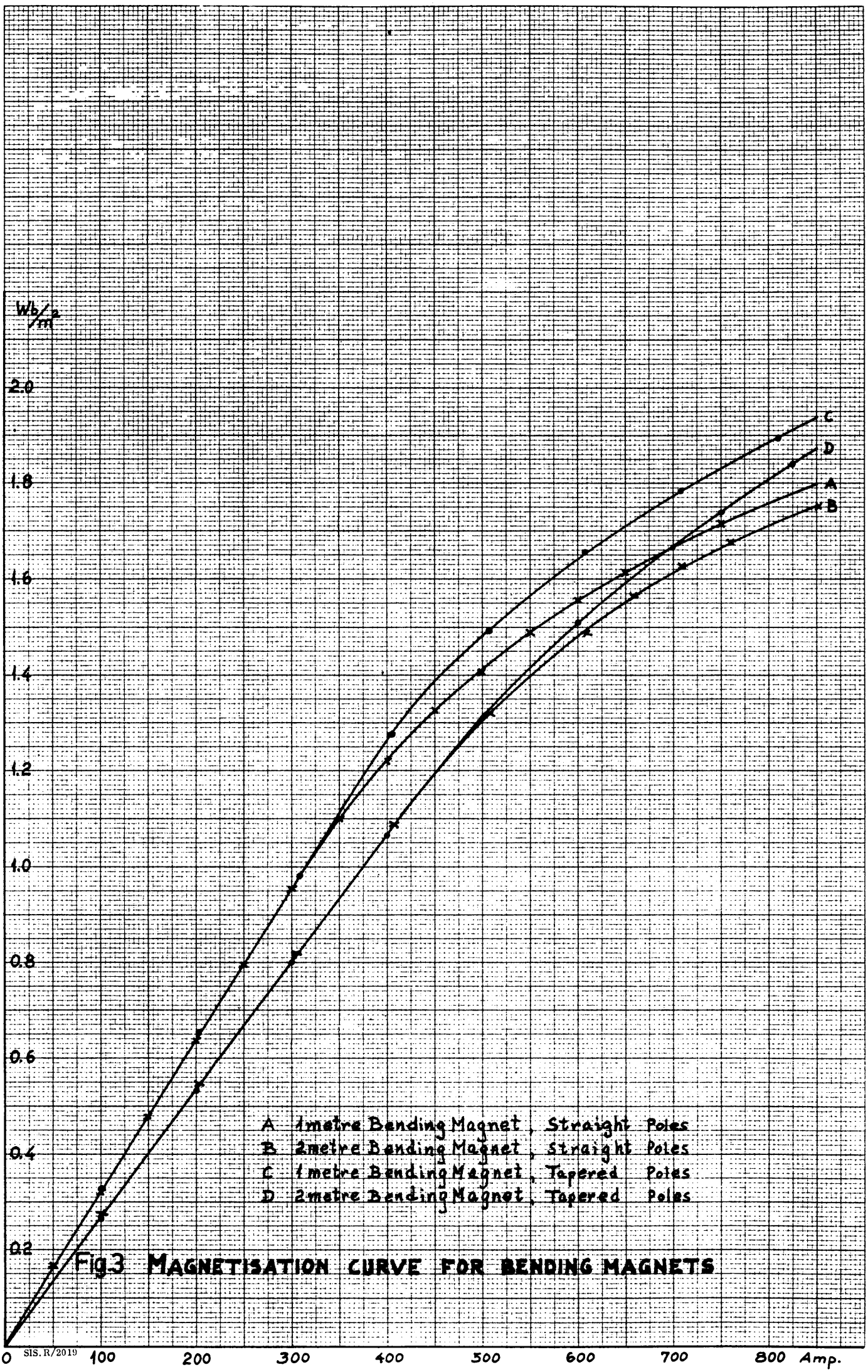

Fig.3 MAGNETISATION CURVE FOR BENDING MAGNETS

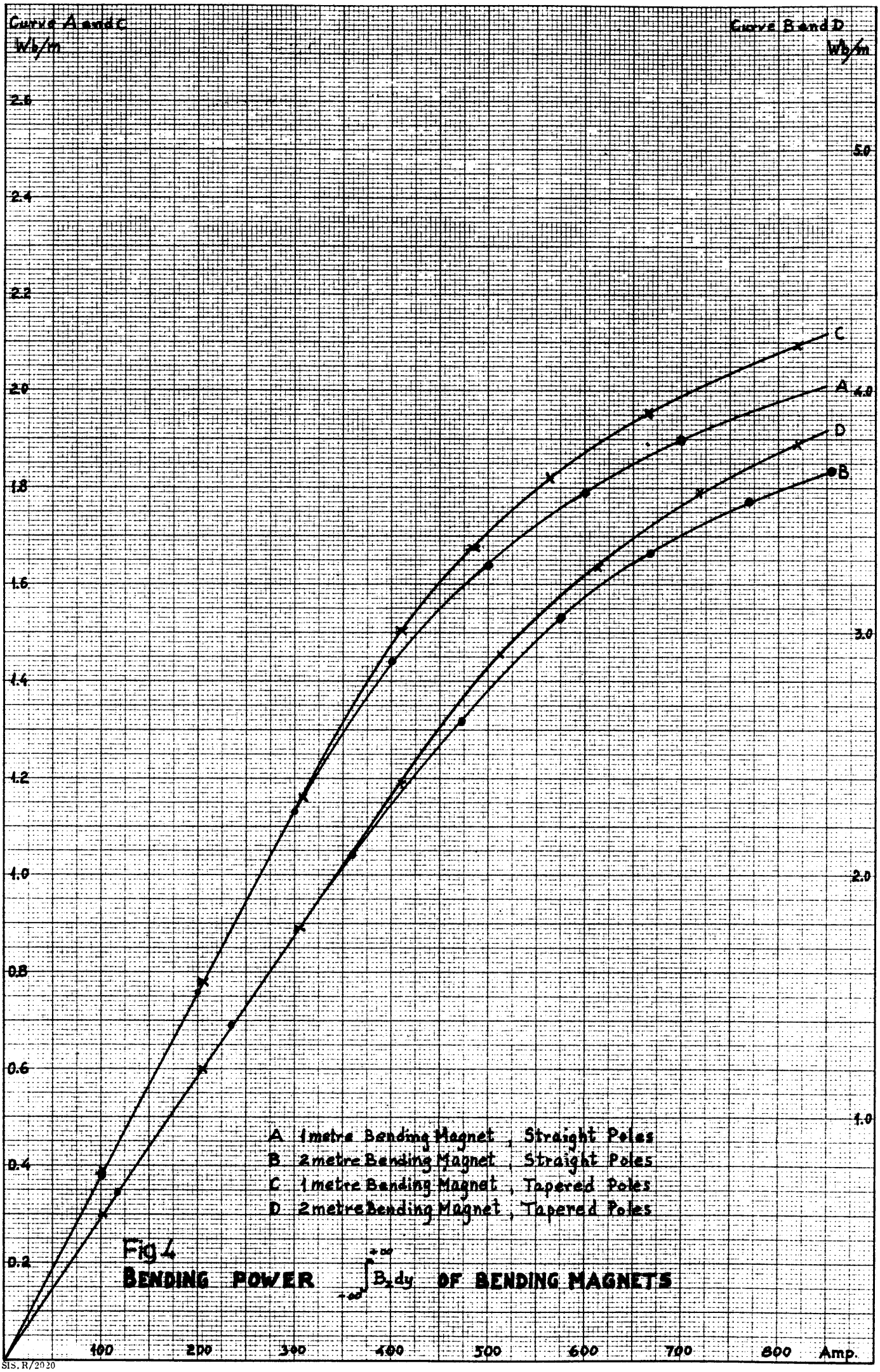

Fig 4

BENDING POWER $\int_{-\infty}^{+\infty} B_z dy$ OF BENDING MAGNETS

SIS. R/2020

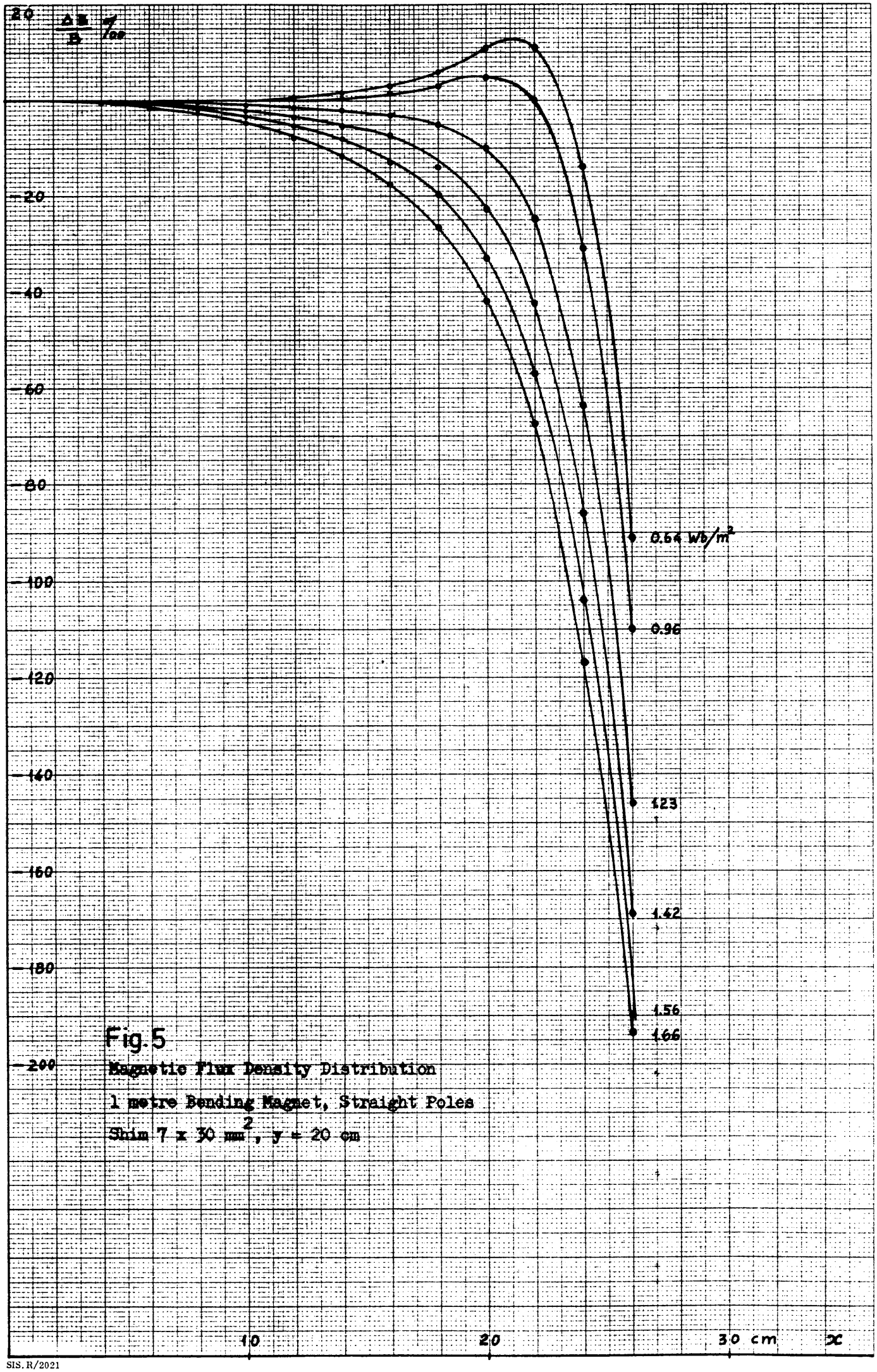

Fig. 5

Magnetic Flux Density Distribution

1 metre Bending Magnet, Straight Poles

Shim 7 x 30 mm², y = 20 cm

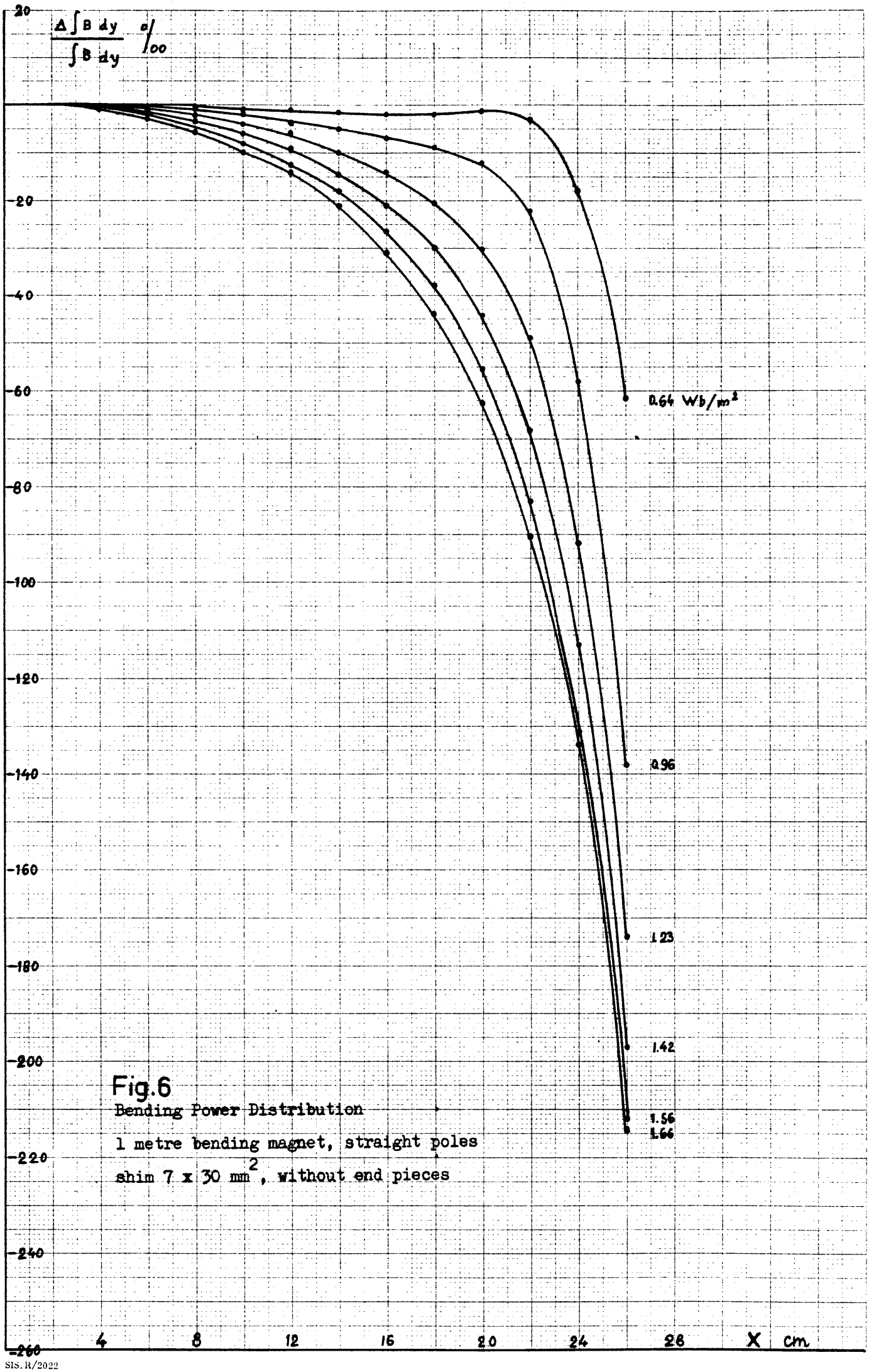

Fig.6

Bending Power Distribution

1 metre bending magnet, straight poles

shim 7 x 30 mm^2, without end pieces

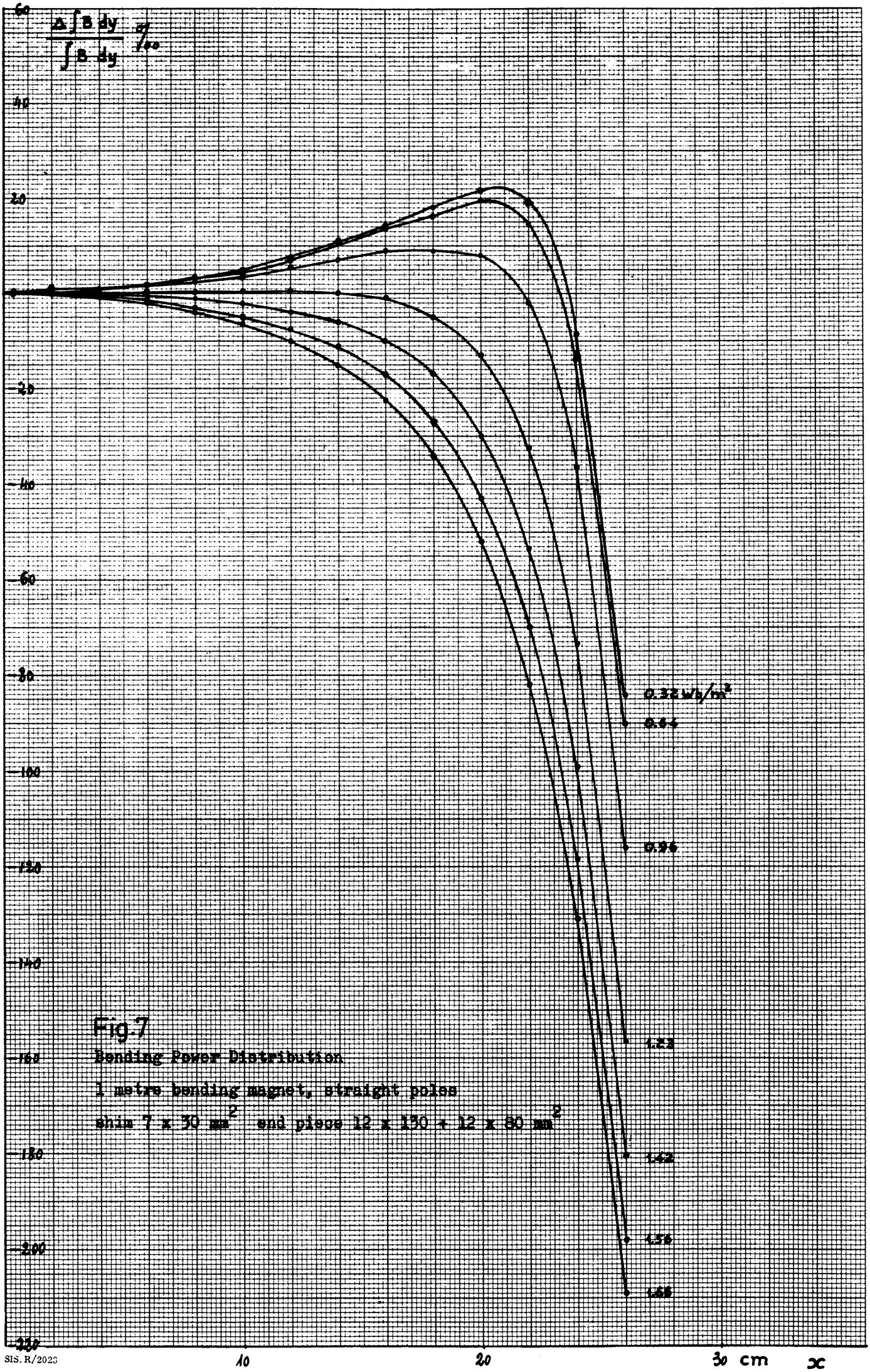

Fig.7

Bending Power Distribution

1 metre bending magnet, straight poles

shim 7 x 30 mm² end piece 12 x 150 + 12 x 80 mm²

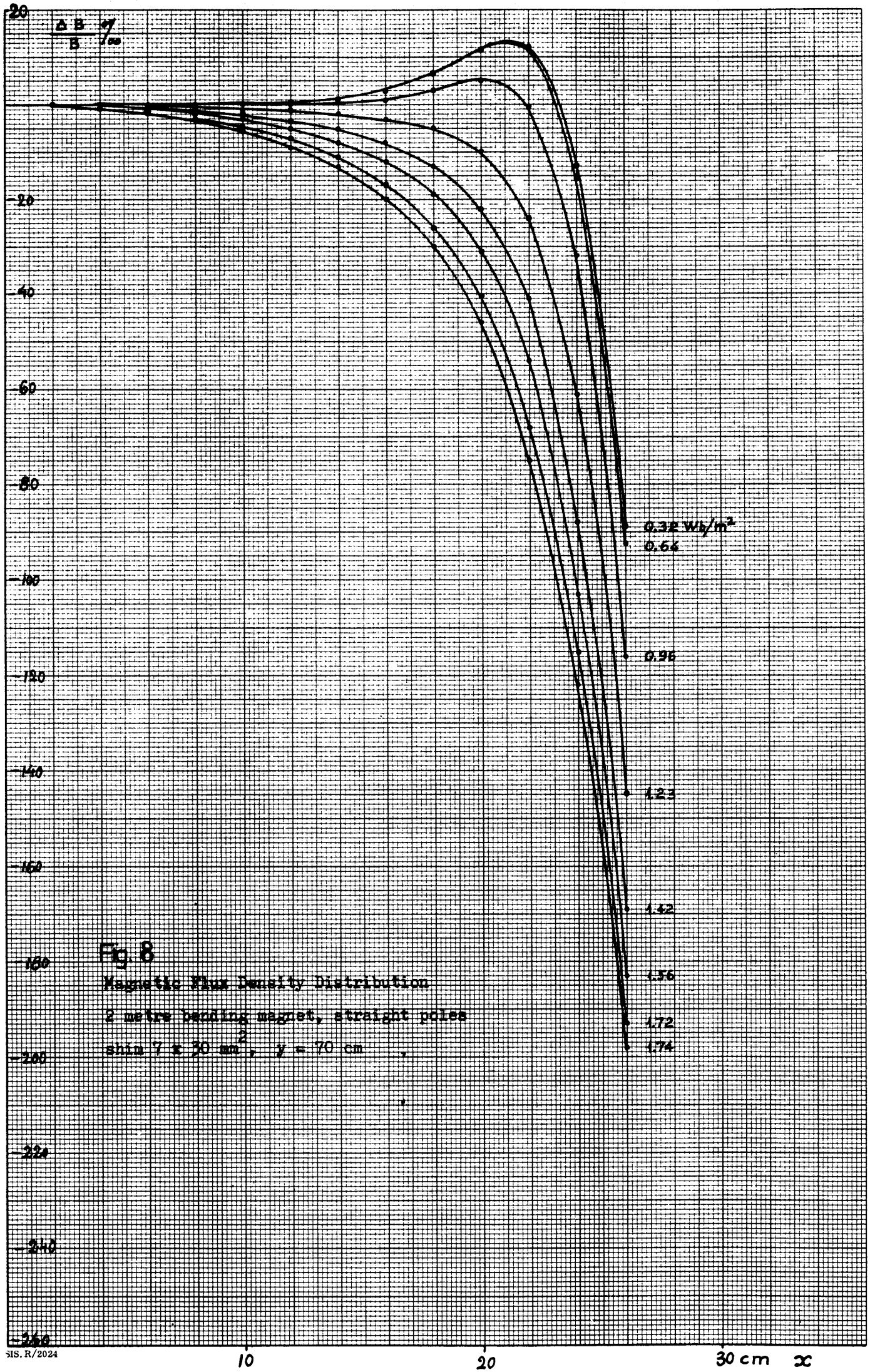

Fig. 8

Magnetic Flux Density Distribution

2 metre bending magnet, straight poles

shim 7 x 30 mm², y = 70 cm

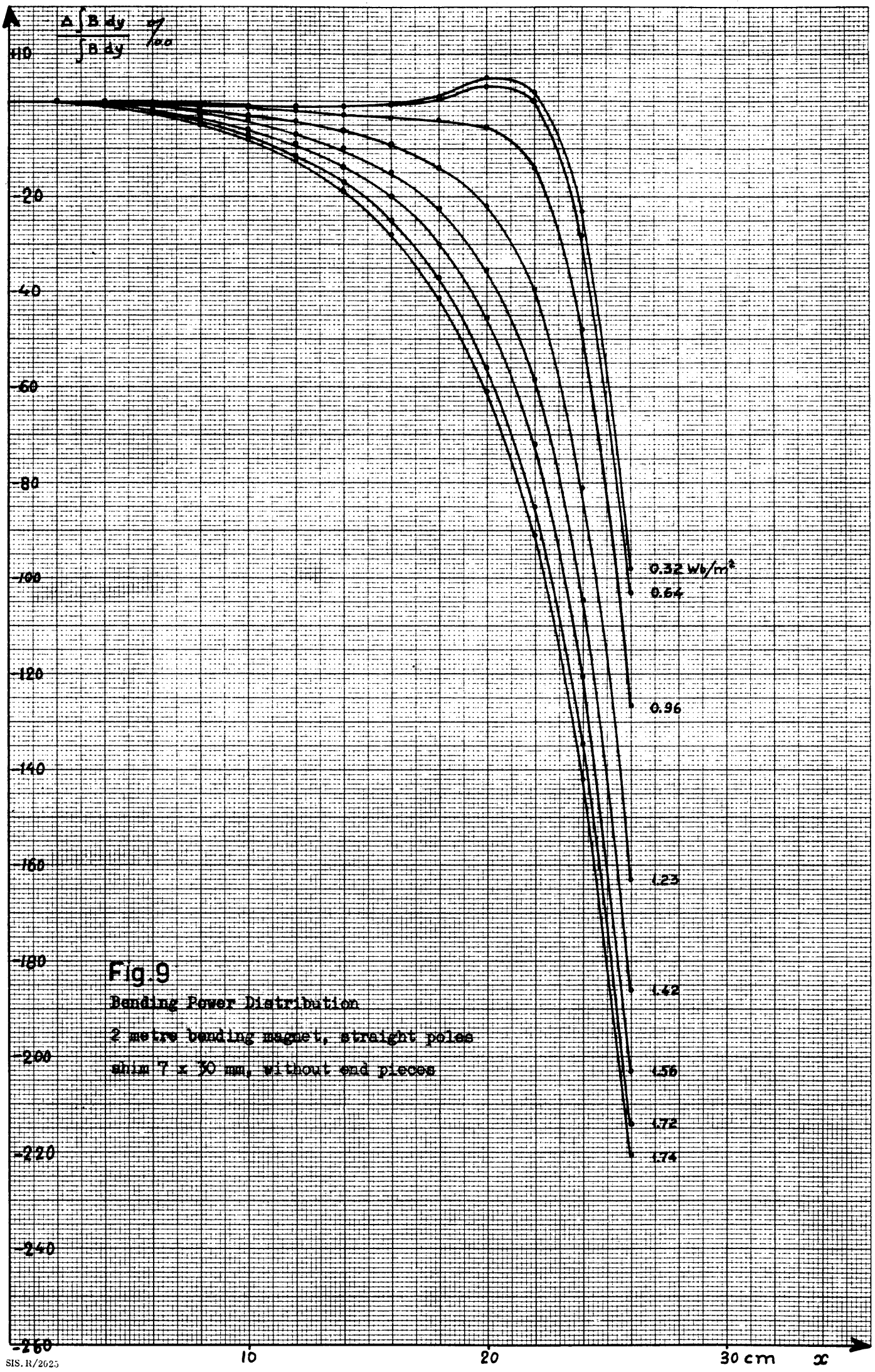

Fig.9

Bending Power Distribution

2 metre bending magnet, straight poles

shim 7 x 30 mm, without end pieces

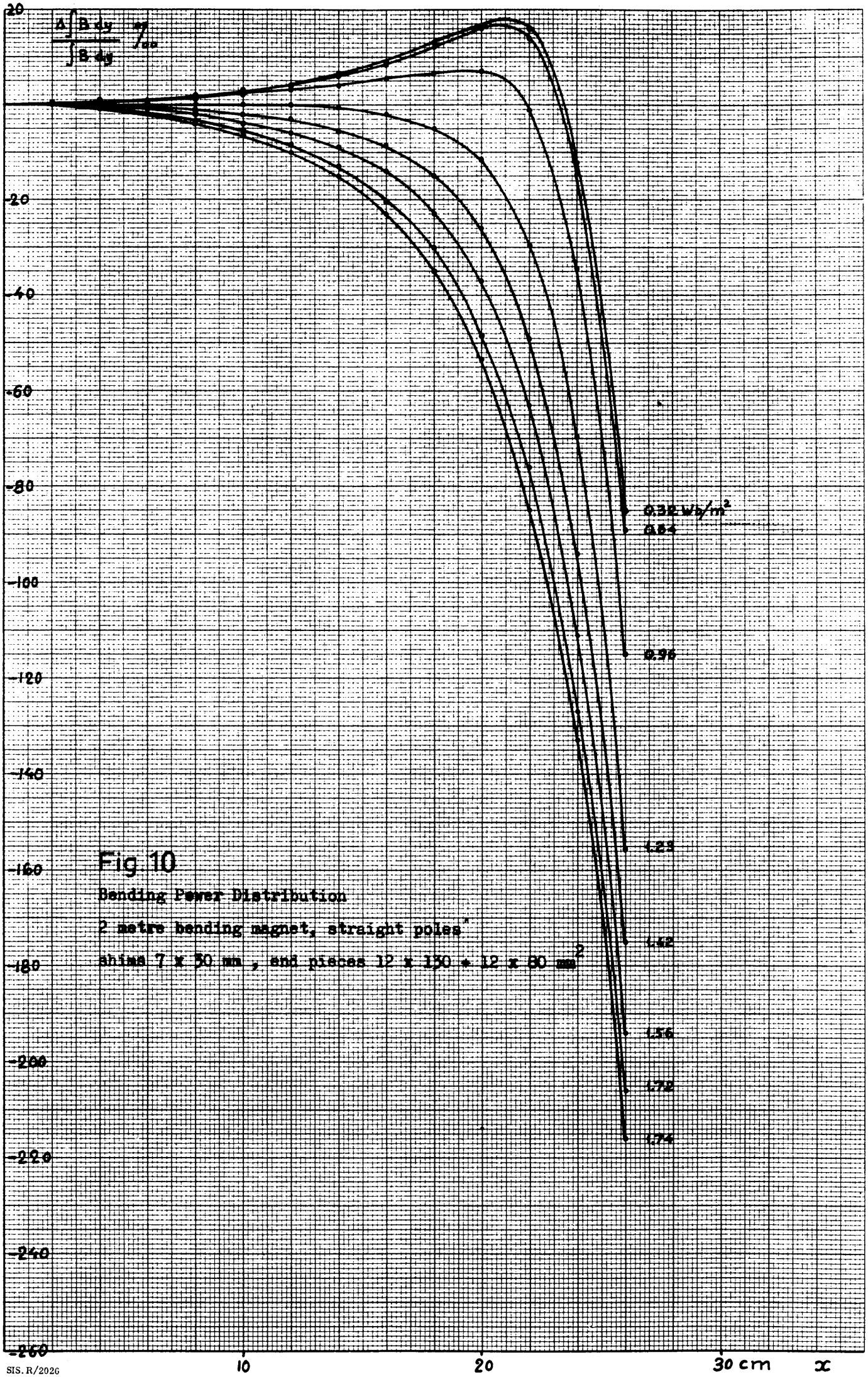

Fig 10

Bending Power Distribution

2 metre bending magnet, straight poles

shims 7 x 30 mm , end pieces 12 x 130 + 12 x 80 mm²

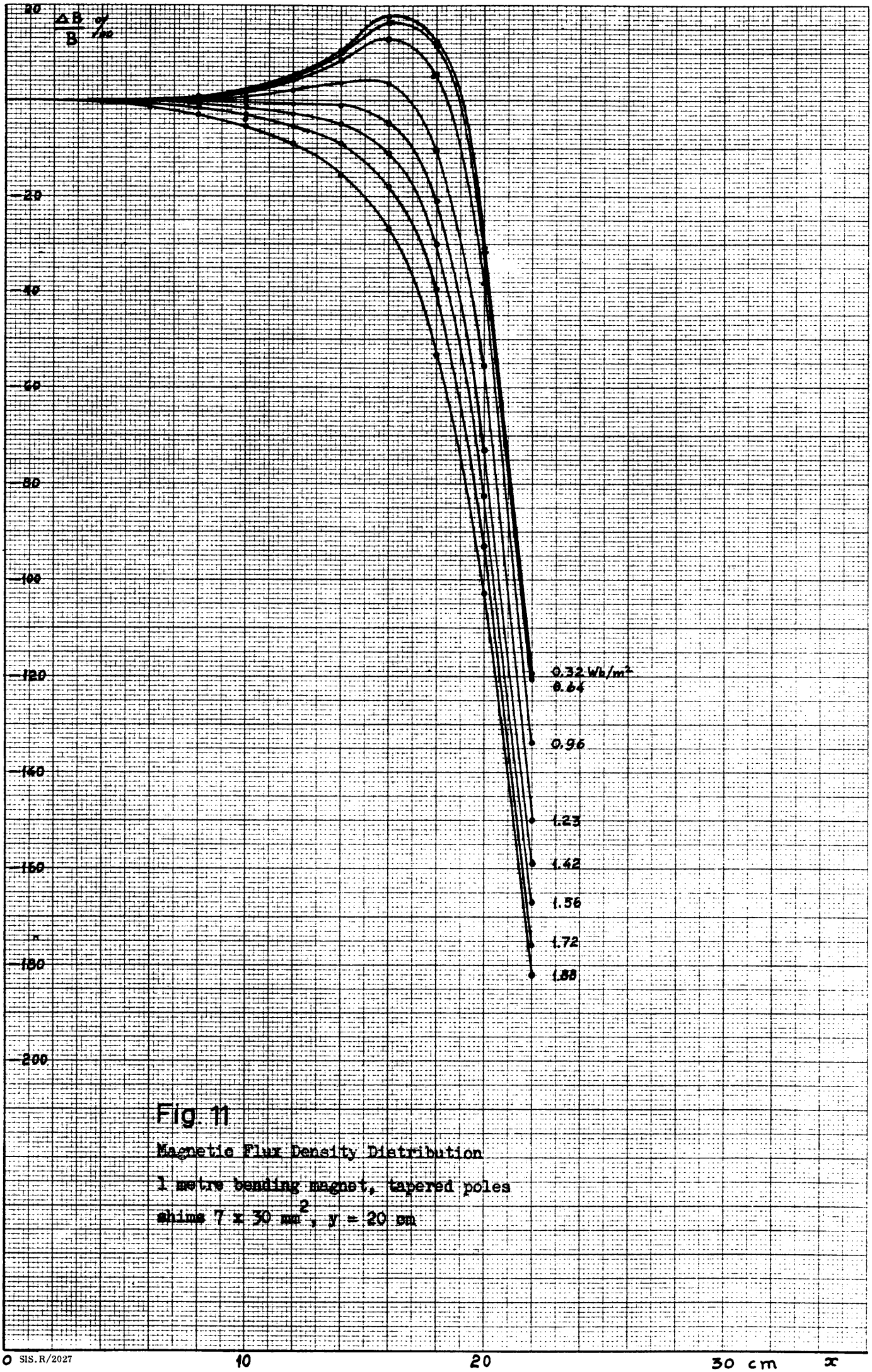

Fig. 11

Magnetic Flux Density Distribution

1 metre bending magnet, tapered poles

shims 7 x 30 mm², y = 20 cm

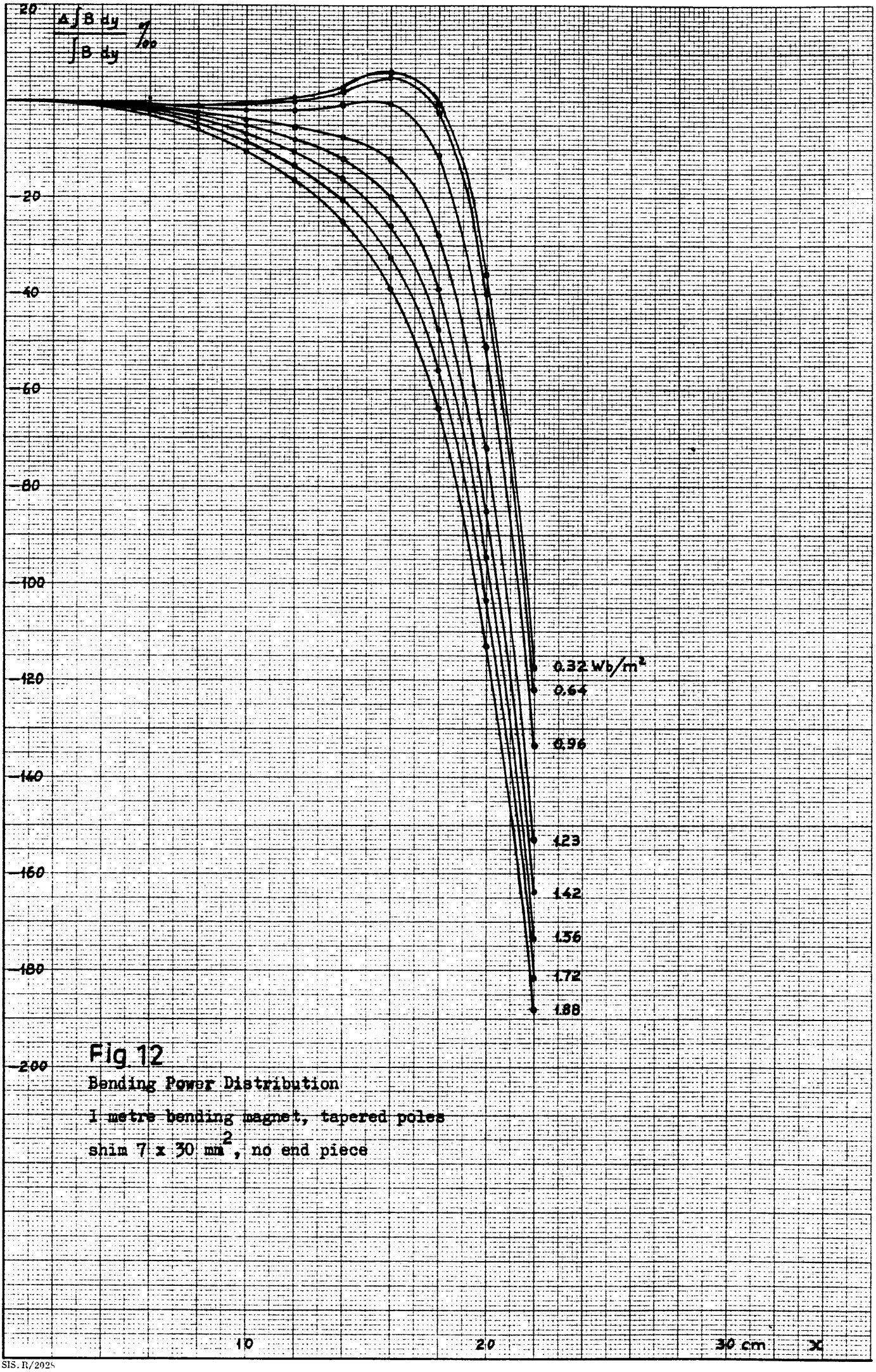

Fig 12

Bending Power Distribution

1 metre bending magnet, tapered poles

shim 7 x 30 mm^2, no end piece

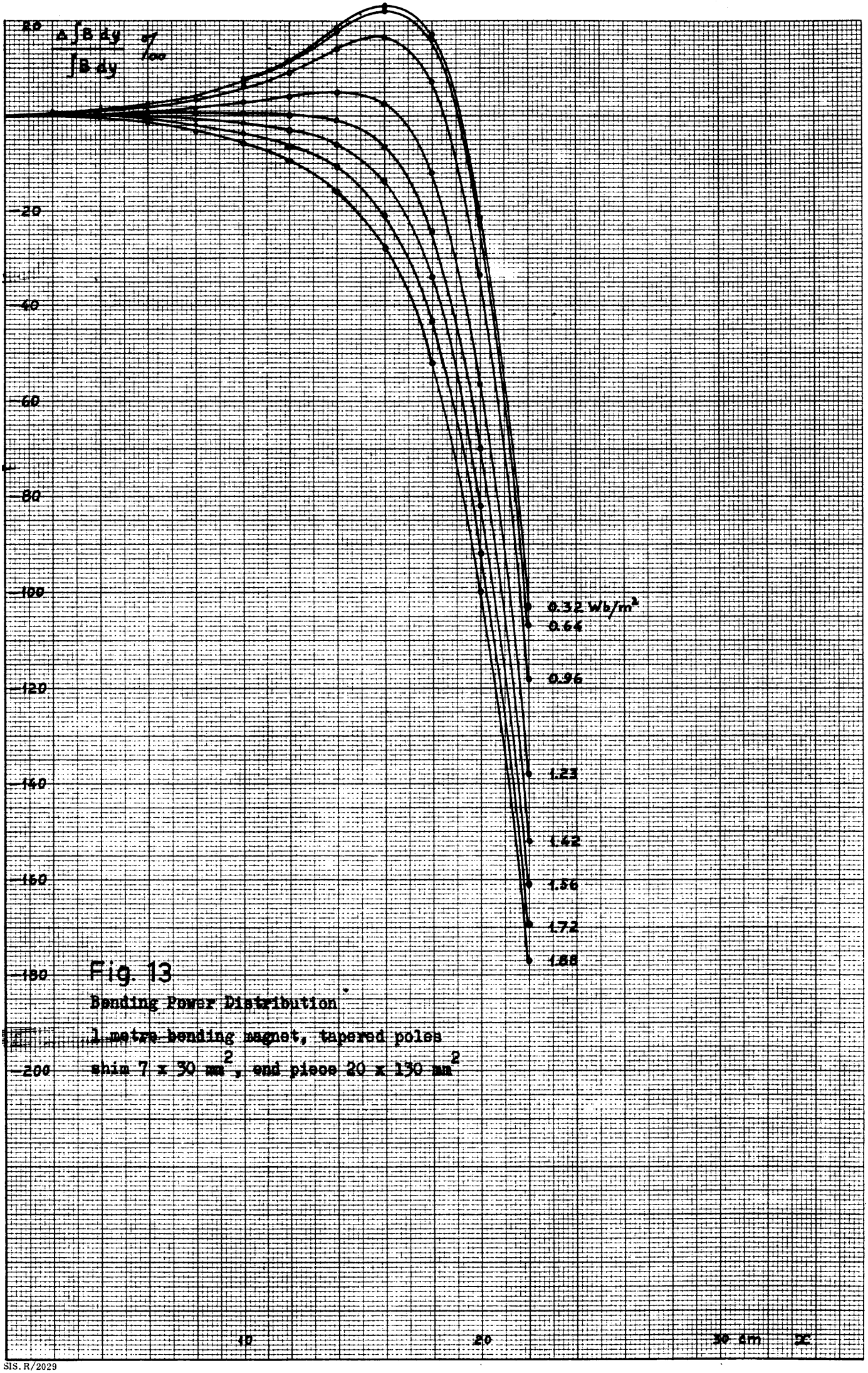

Fig. 13

Bending Power Distribution

1 metre bending magnet, tapered poles

shim 7 x 30 mm², end piece 20 x 130 mm²

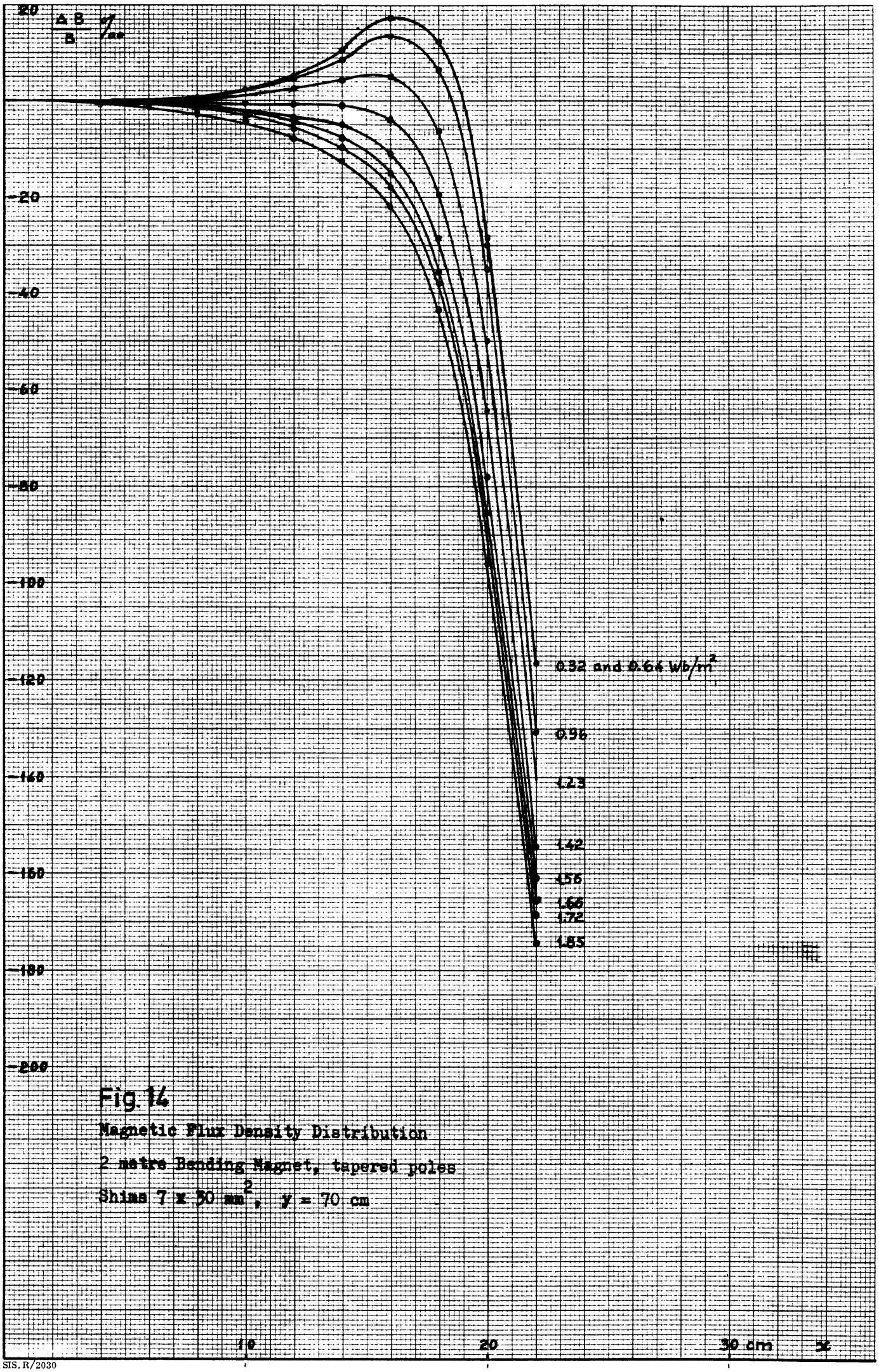

Fig. 14

Magnetic Flux Density Distribution

2 metre Bending Magnet, tapered poles

Shims 7 x 50 mm², y = 70 cm

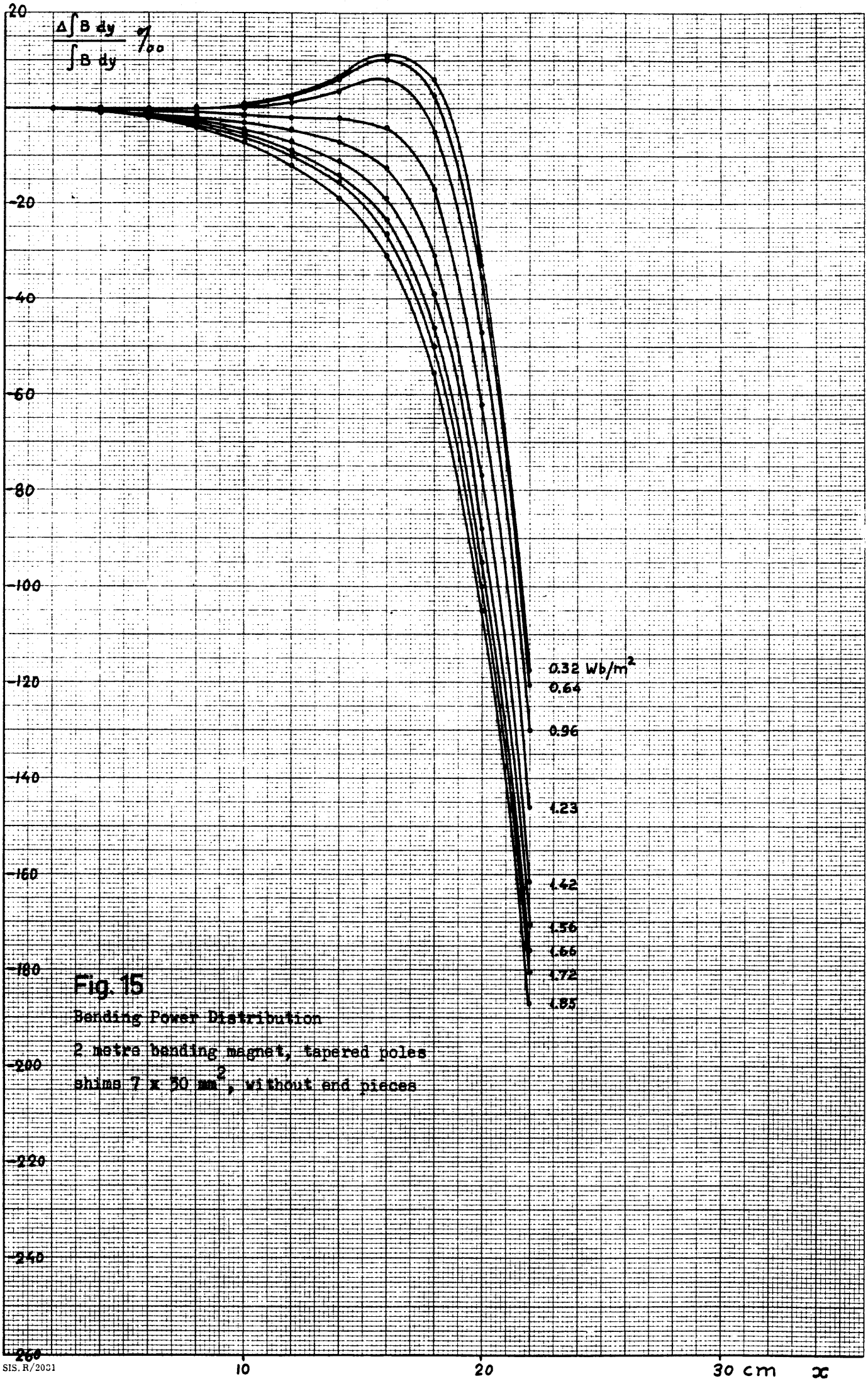

Fig. 15

Bending Power Distribution

2 metre bending magnet, tapered poles

shims 7 x 50 mm², without end pieces

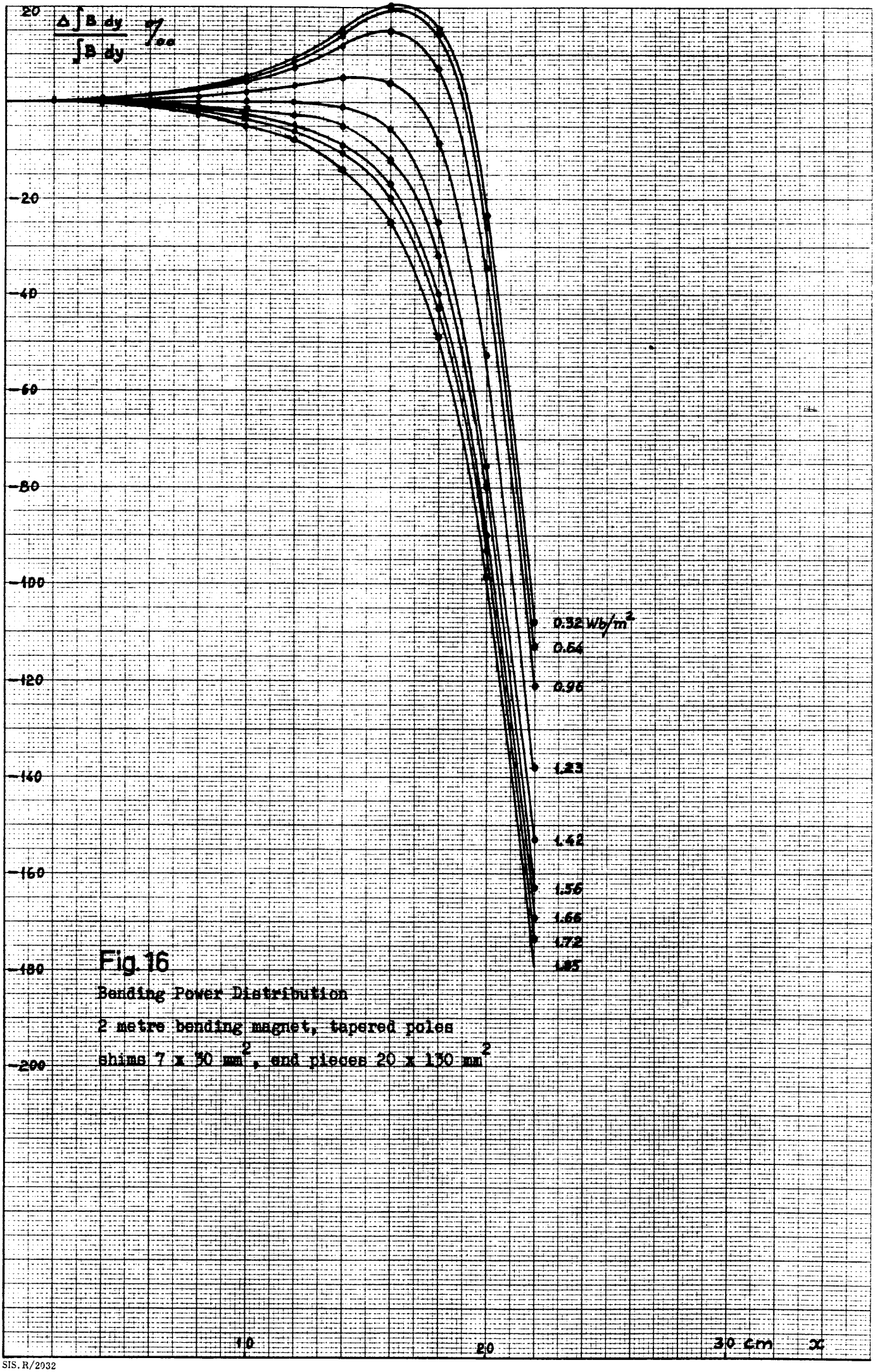

Fig. 16

Bending Power Distribution

2 metre bending magnet, tapered poles

shims 7 x 50 mm², and pieces 20 x 150 mm²

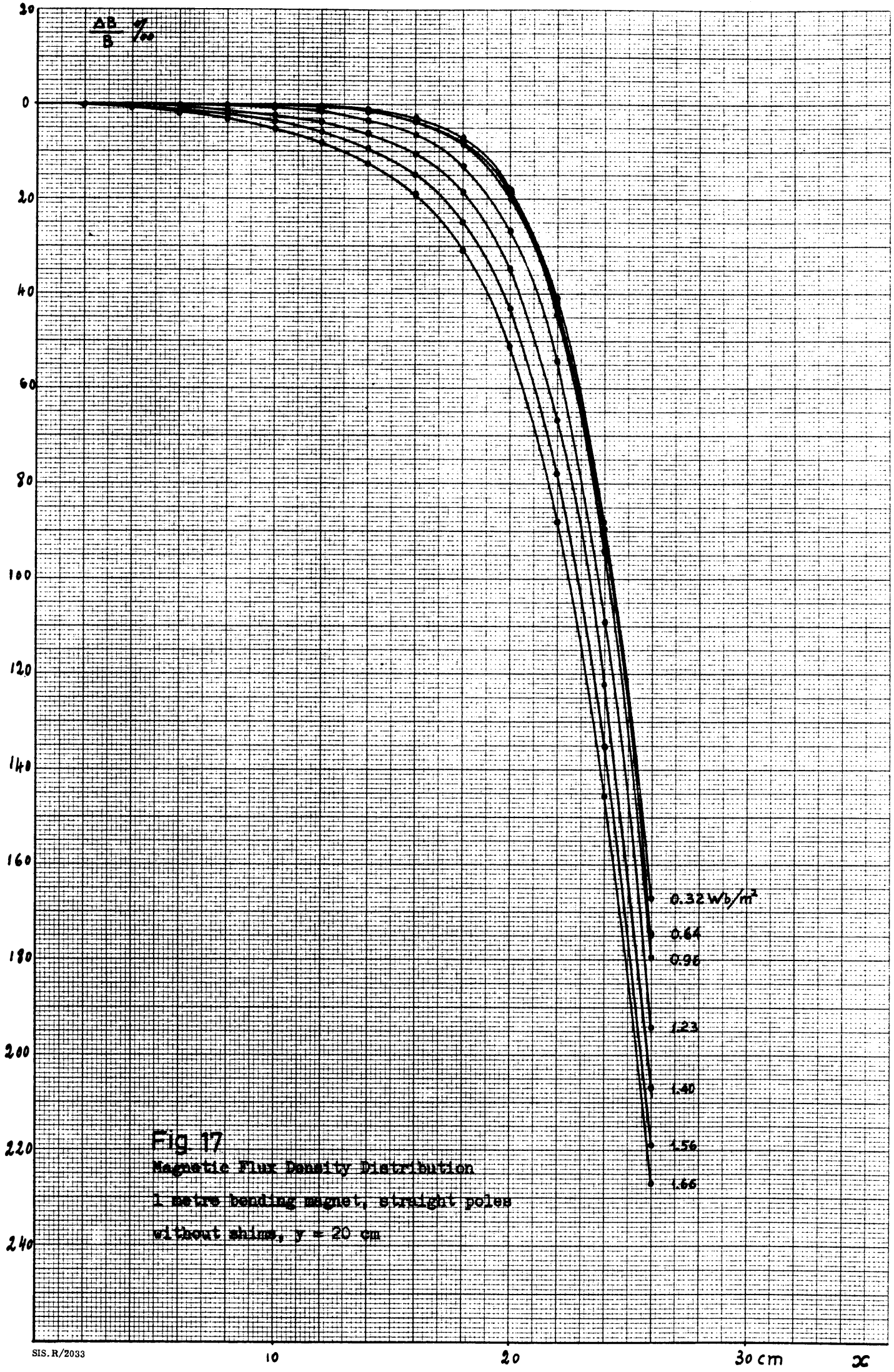

Fig. 17

Magnetic Flux Density Distribution

1 metre bending magnet, straight poles

without shims, y = 20 cm

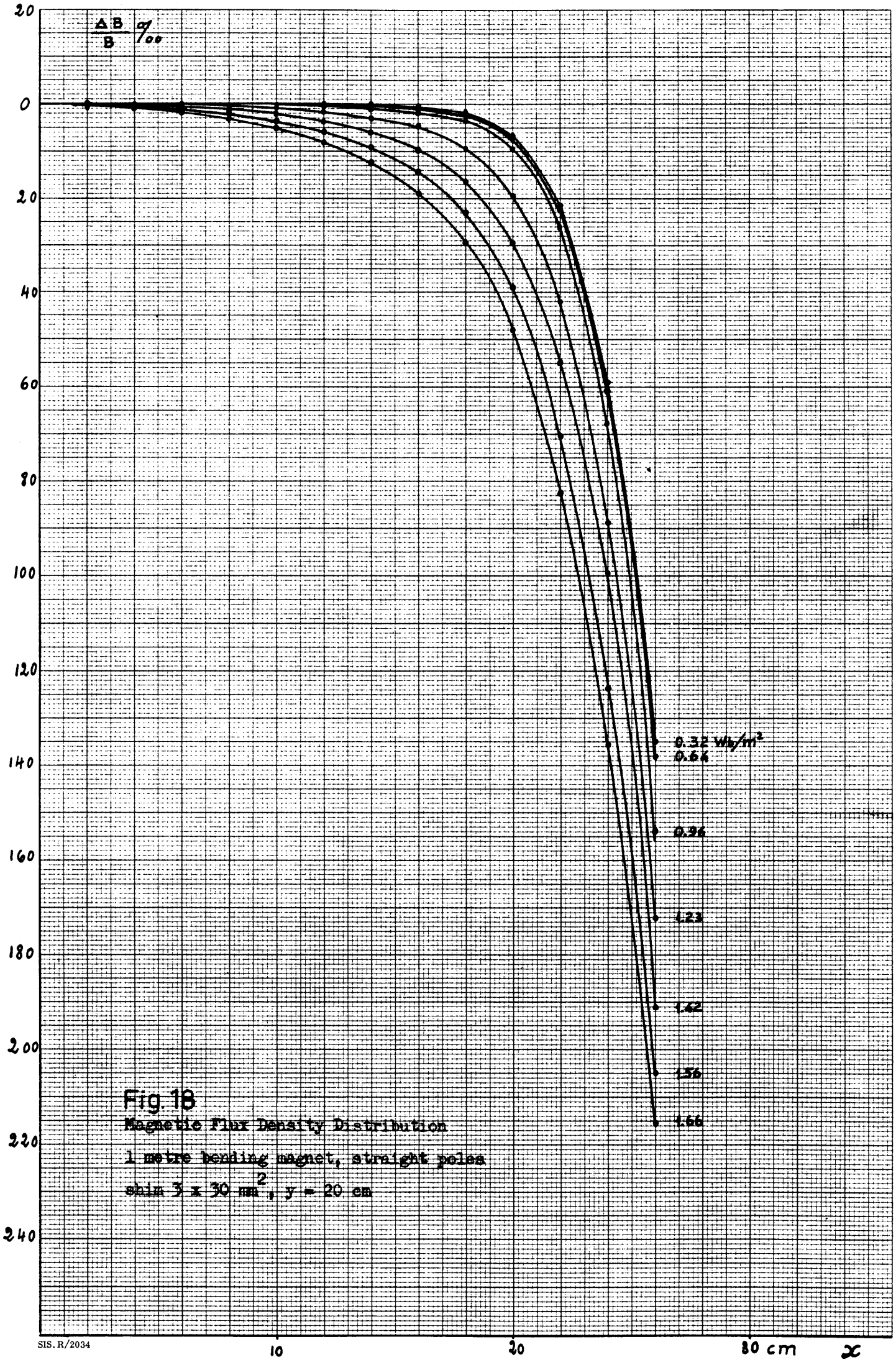

Fig. 18

Magnetic Flux Density Distribution

1 metre bending magnet, straight poles

shim 3 x 30 mm², y = 20 cm

SIS. R/2034

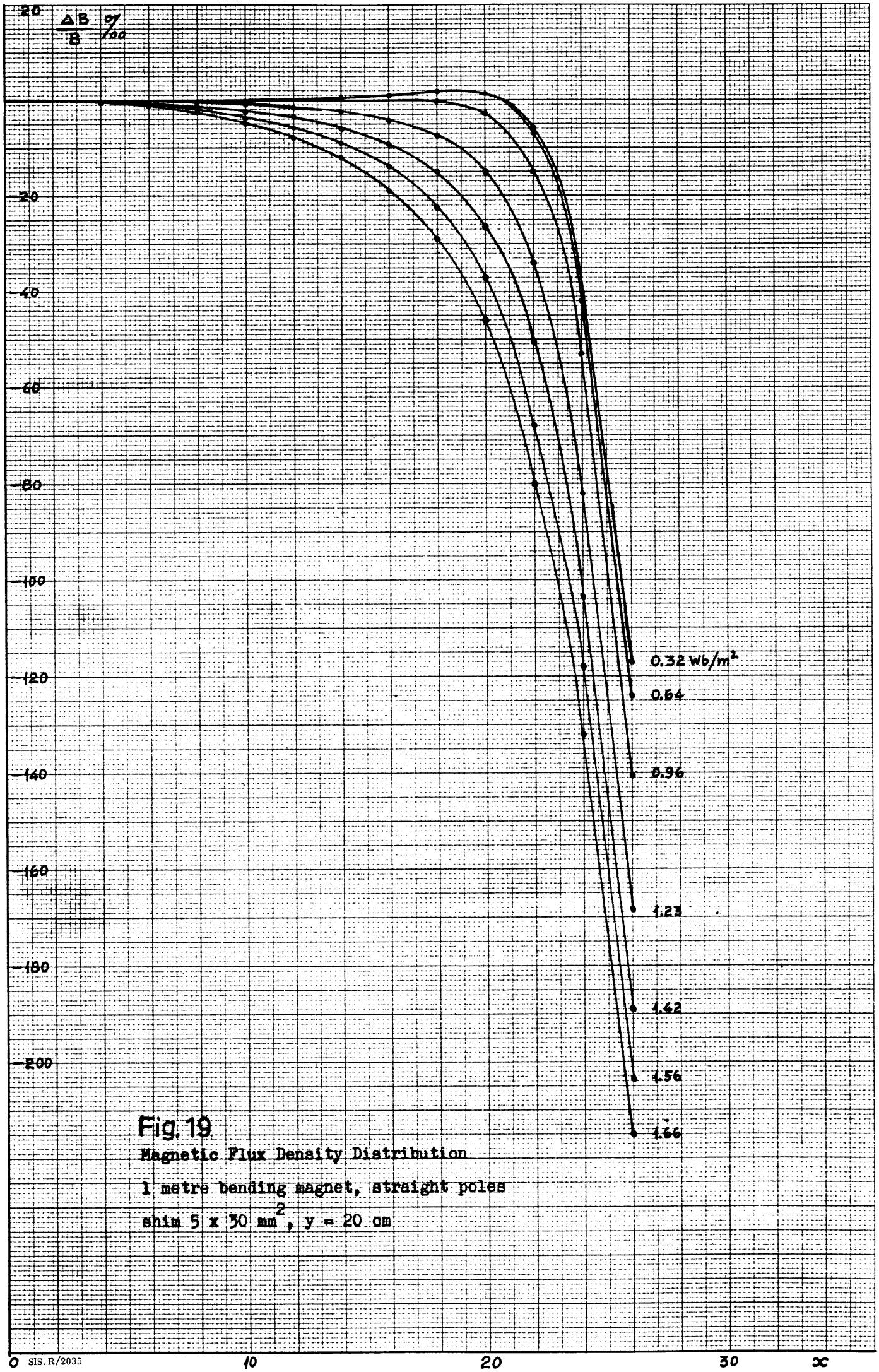

Fig. 19

Magnetic Flux Density Distribution

1 metre bending magnet, straight poles

shim 5 x 50 mm^2, y = 20 cm

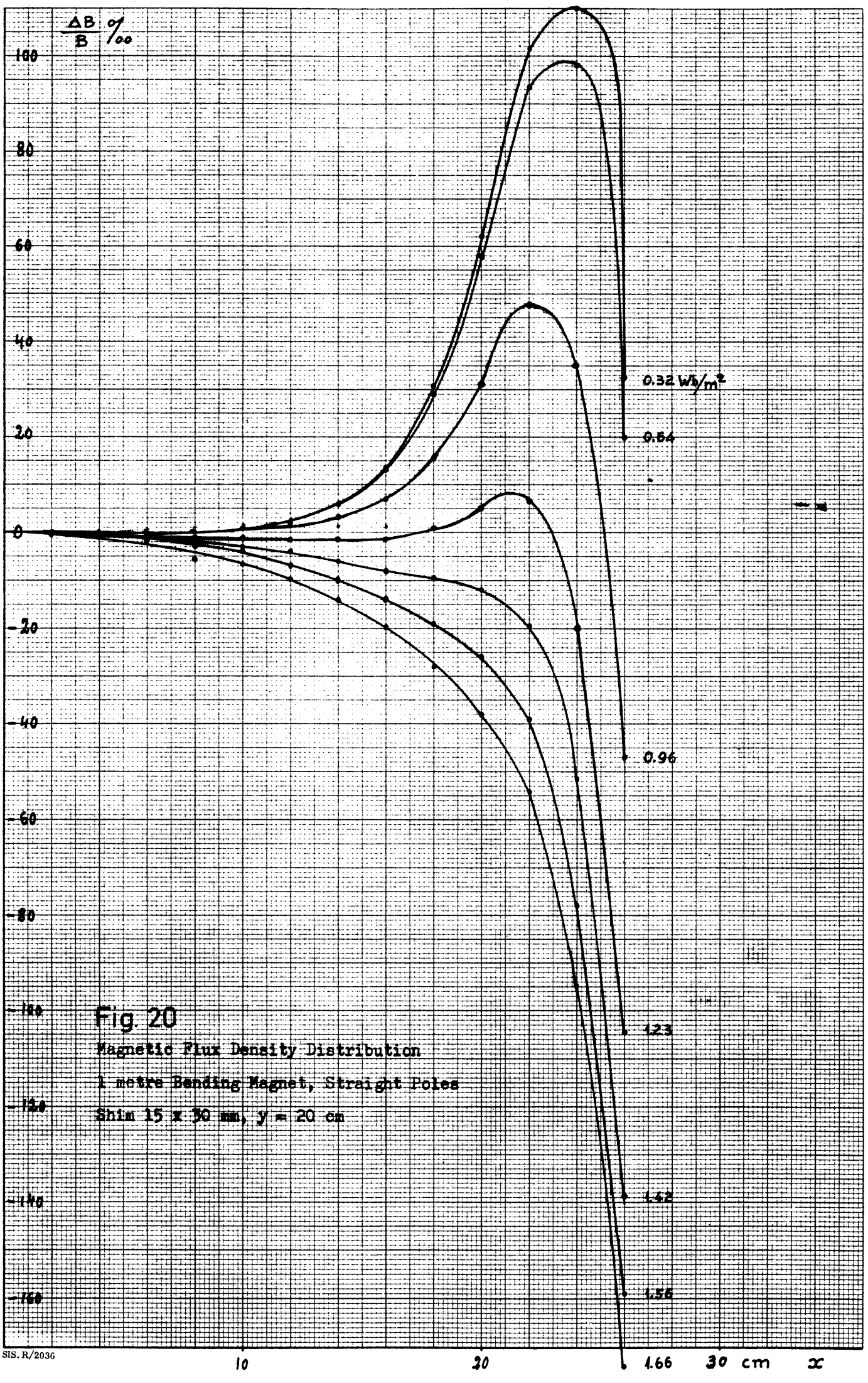

Fig. 20

Magnetic Flux Density Distribution

1 metre Bending Magnet, Straight Poles

Shim 15 x 30 mm, y = 20 cm

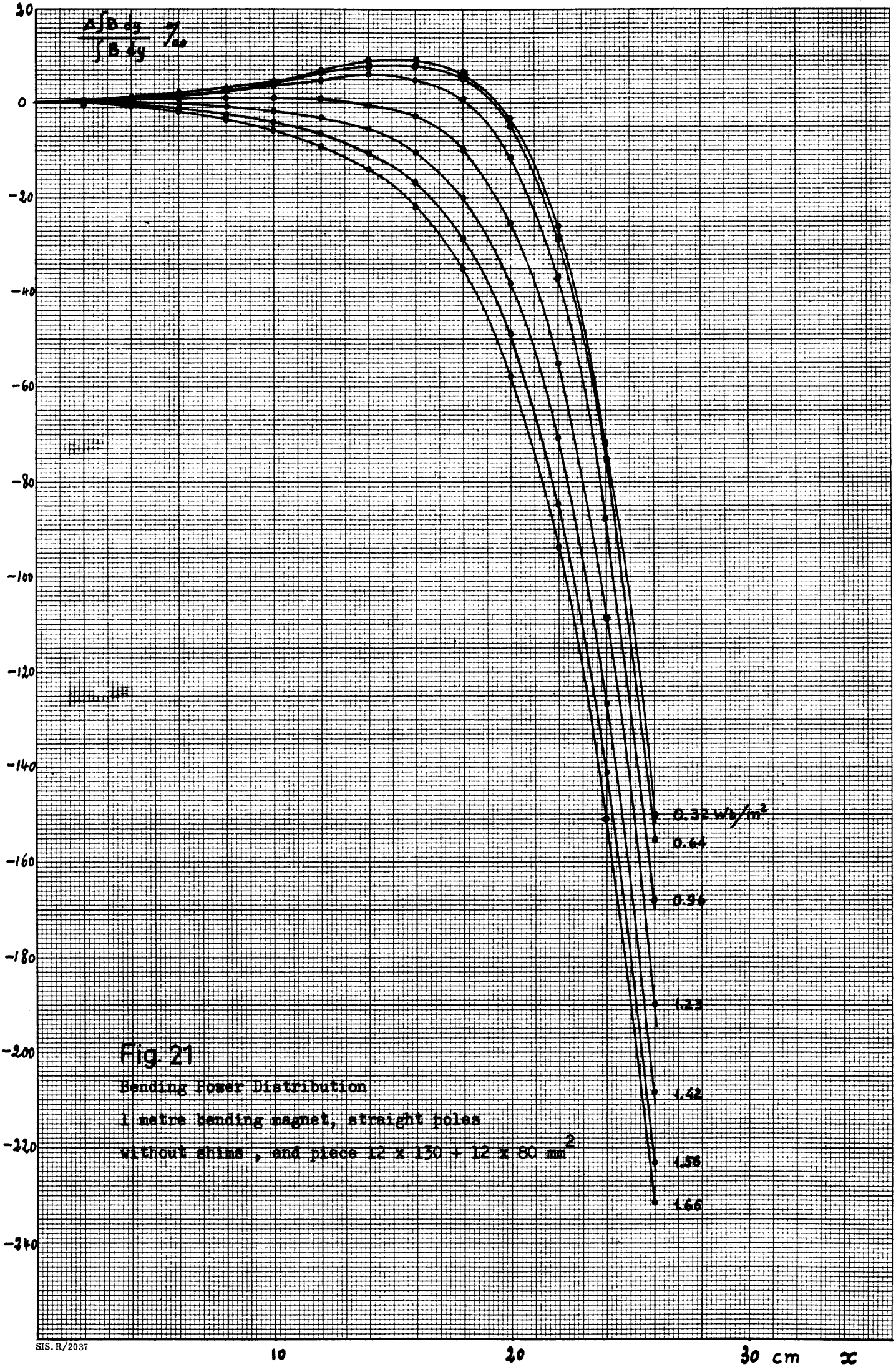

Fig. 21

Bending Power Distribution

1 metre bending magnet, straight poles

without shims , end piece 12 x 150 + 12 x 80 mm²

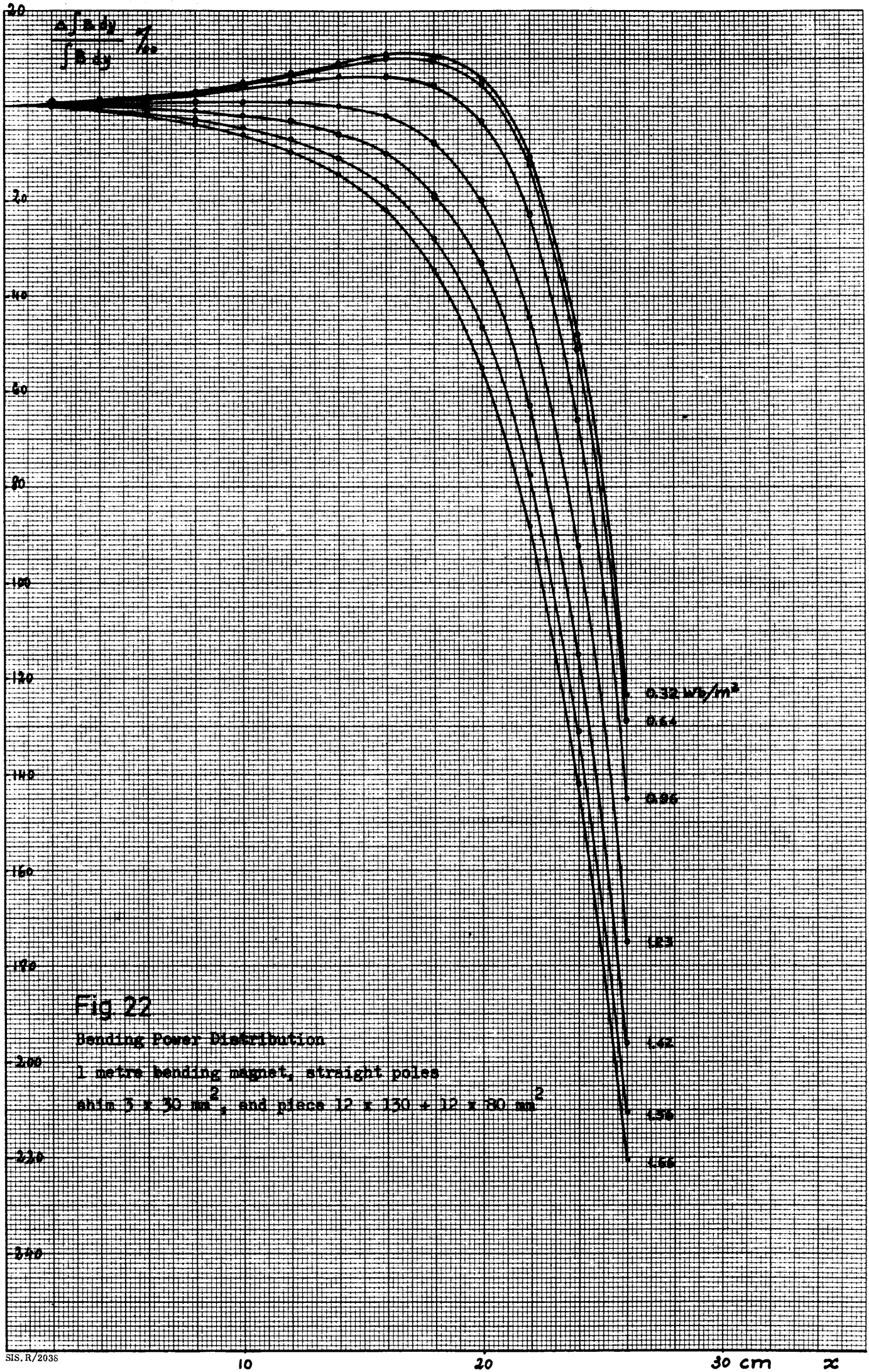

Fig 22

Bending Power Distribution

1 metre bending magnet, straight poles

shim 3 x 30 mm², end piece 12 x 130 + 12 x 80 mm²

SIS. R/2038

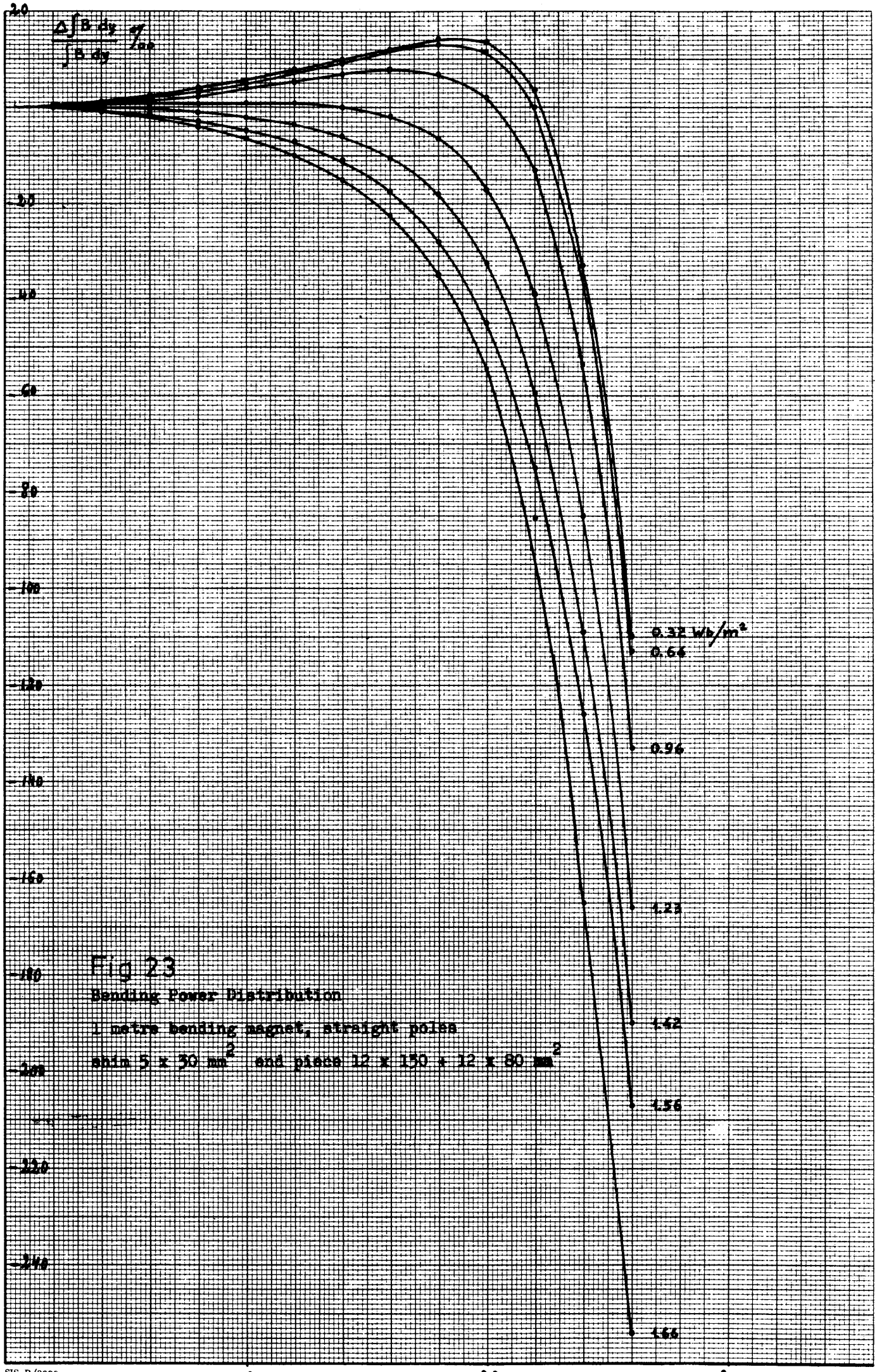

Fig 23

Bending Power Distribution

1 metre bending magnet, straight poles

shim 5 x 30 mm² end piece 12 x 150 + 12 x 80 mm²

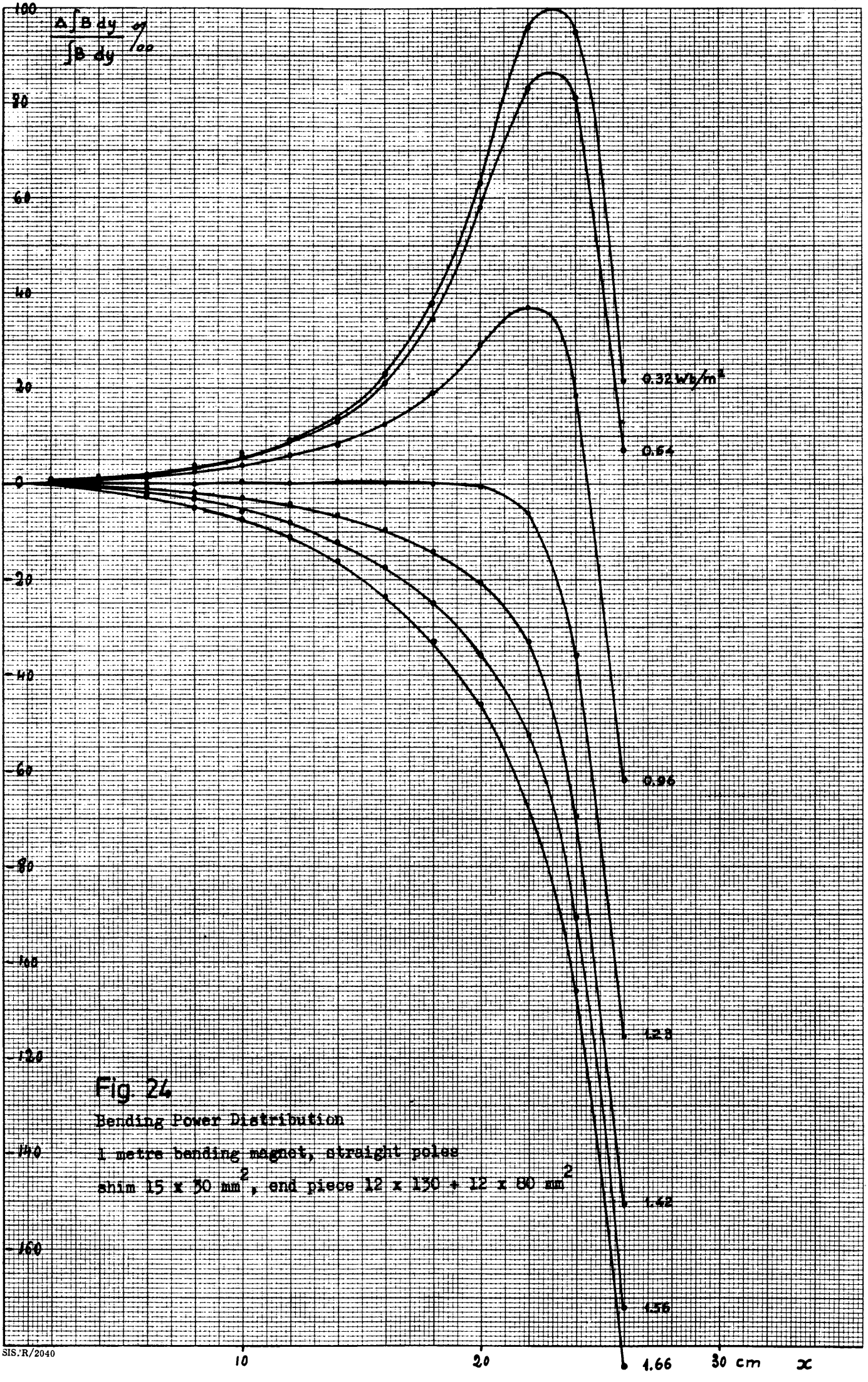

Fig. 24

Bending Power Distribution

1 metre bending magnet, straight poles

shim 15 x 50 mm^2, end piece 12 x 130 + 12 x 80 mm^2

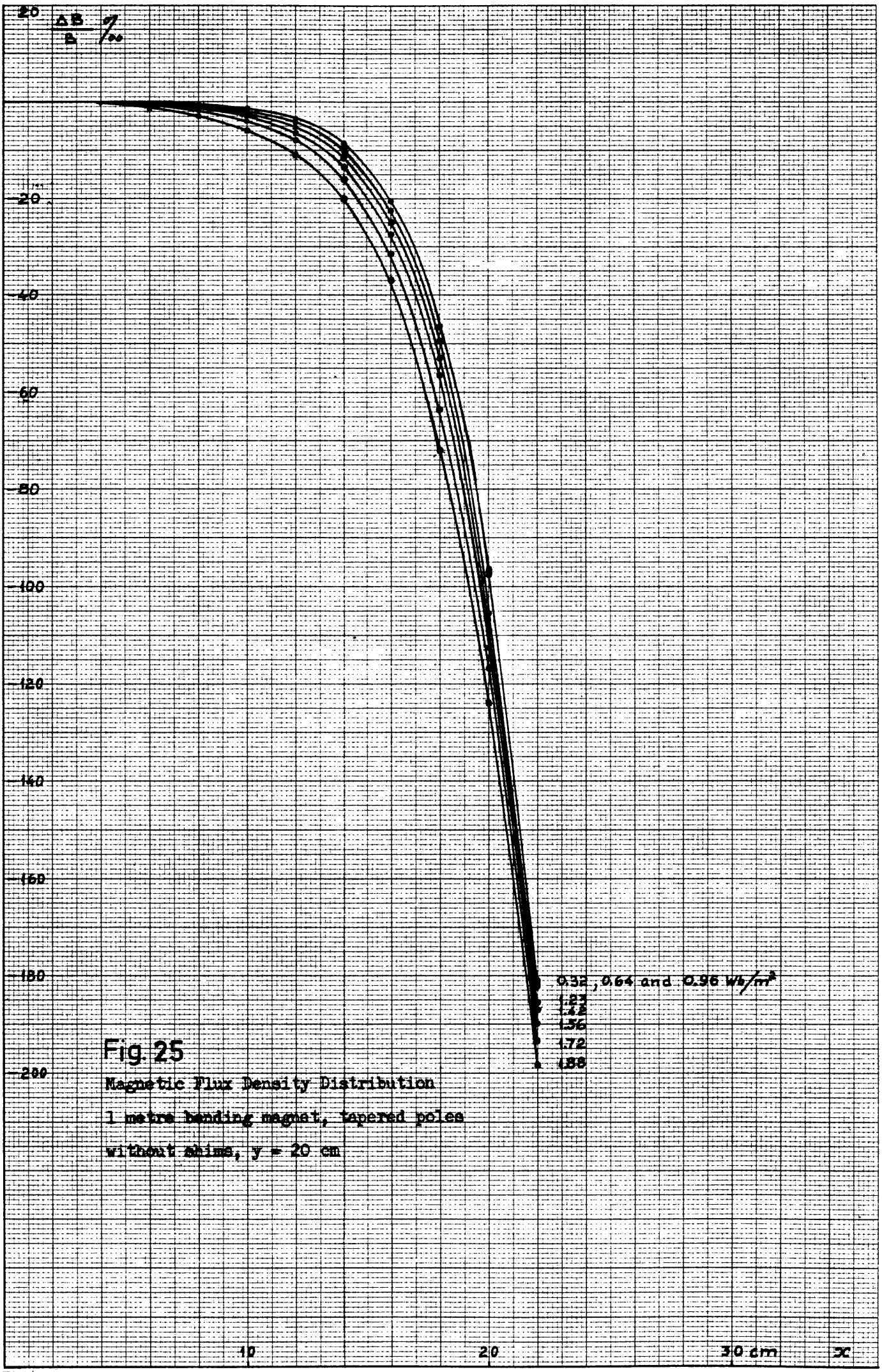

Fig. 25

Magnetic Flux Density Distribution

1 metre bending magnet, tapered poles

without shims, y = 20 cm

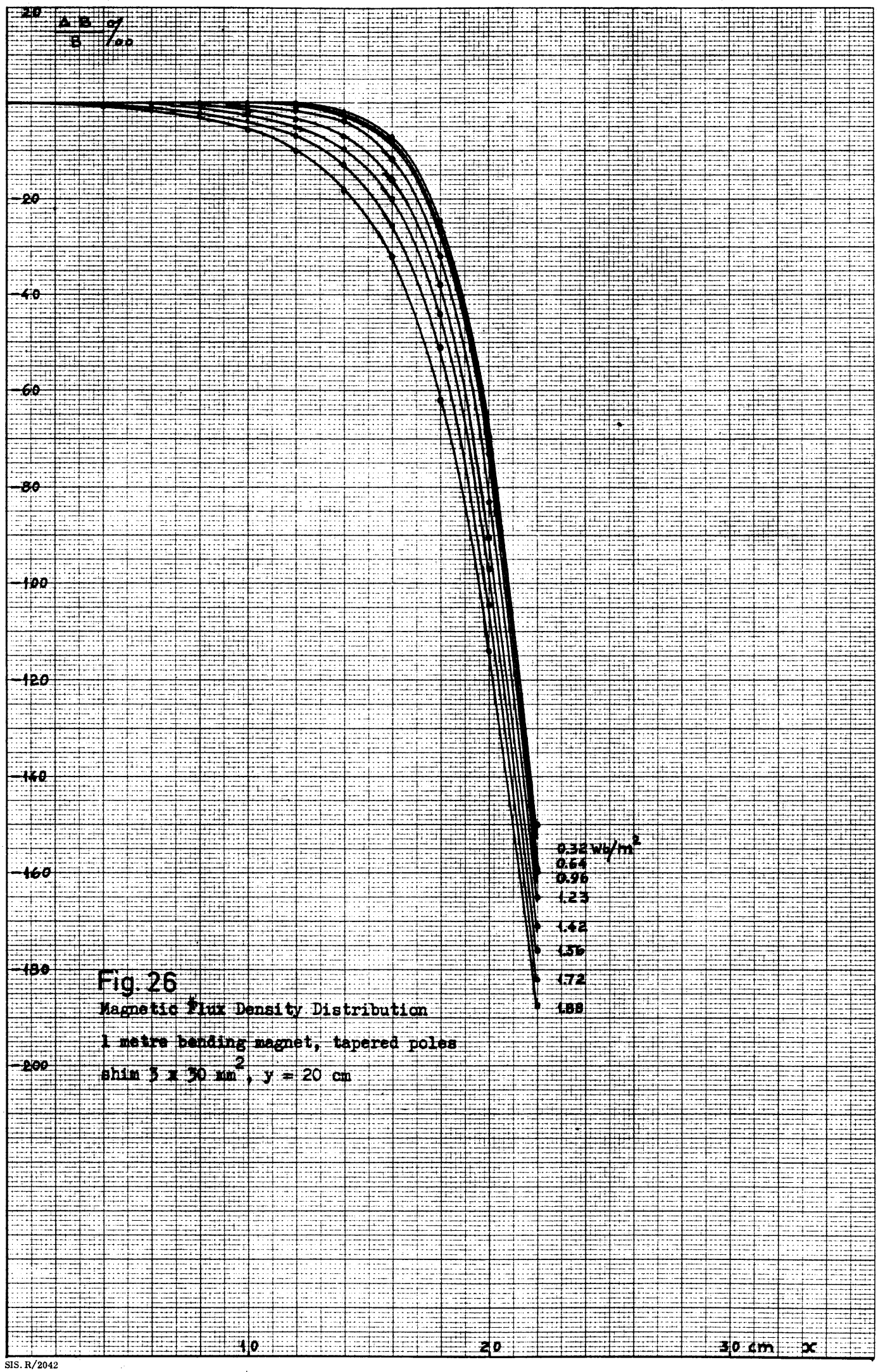

Fig. 26

Magnetic Flux Density Distribution

1 metre bending magnet, tapered poles

shim 3 x 50 mm², y = 20 cm

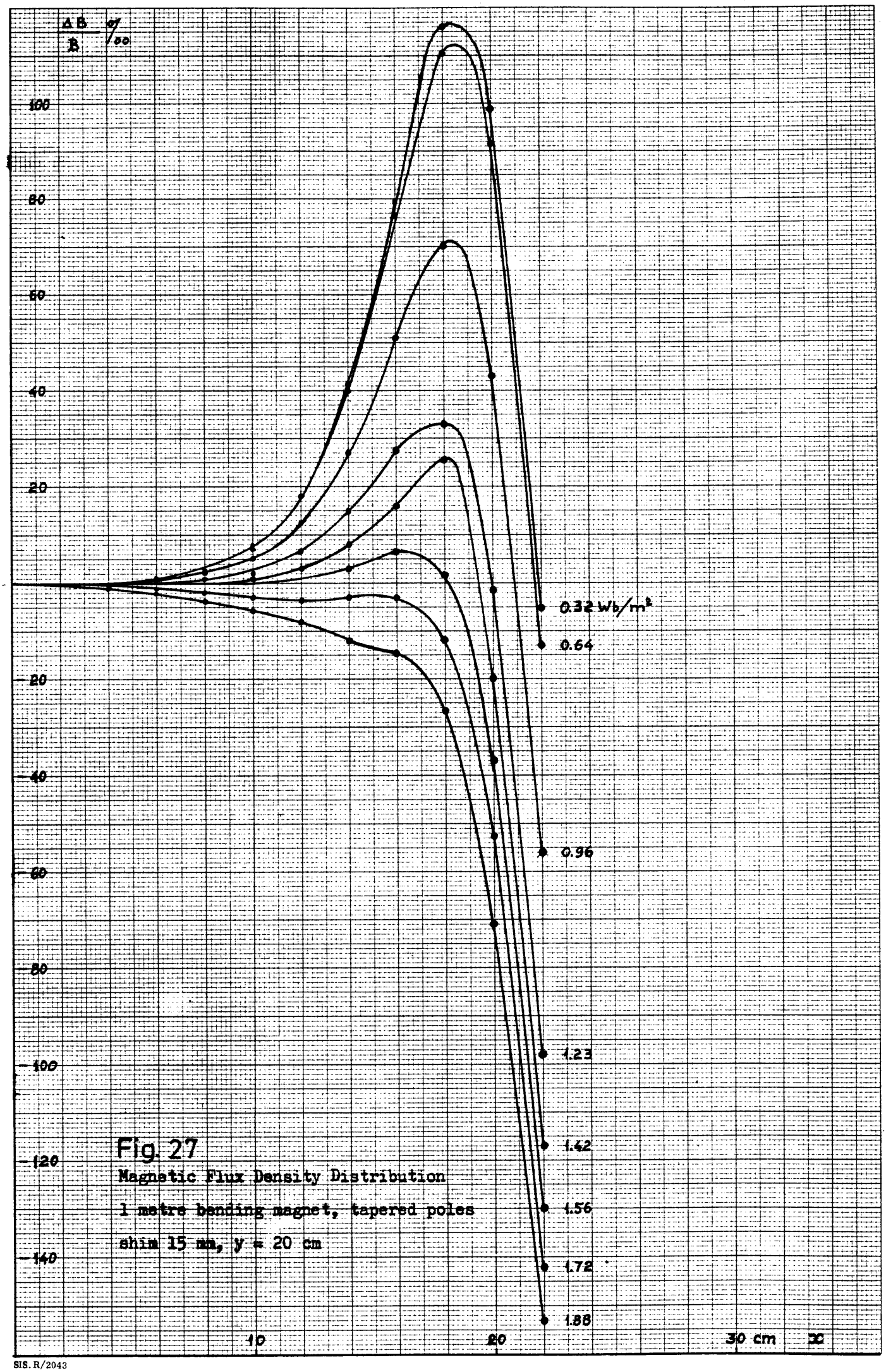

Fig. 27

Magnetic Flux Density Distribution

1 metre bending magnet, tapered poles

shim 15 mm, y = 20 cm

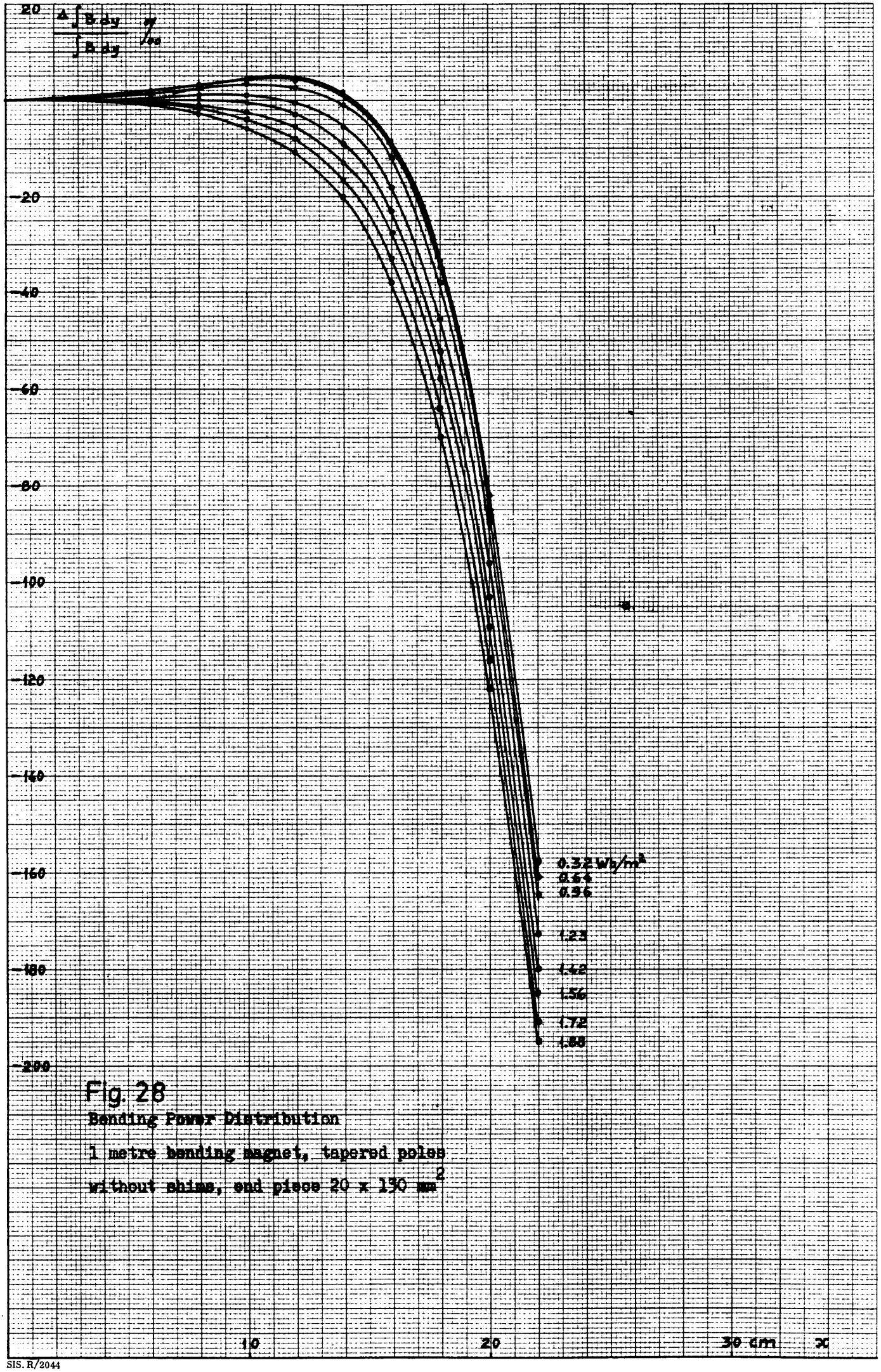

Fig. 28

Bending Power Distribution

1 metre bending magnet, tapered poles without shims, end piece 20 x 130 mm²

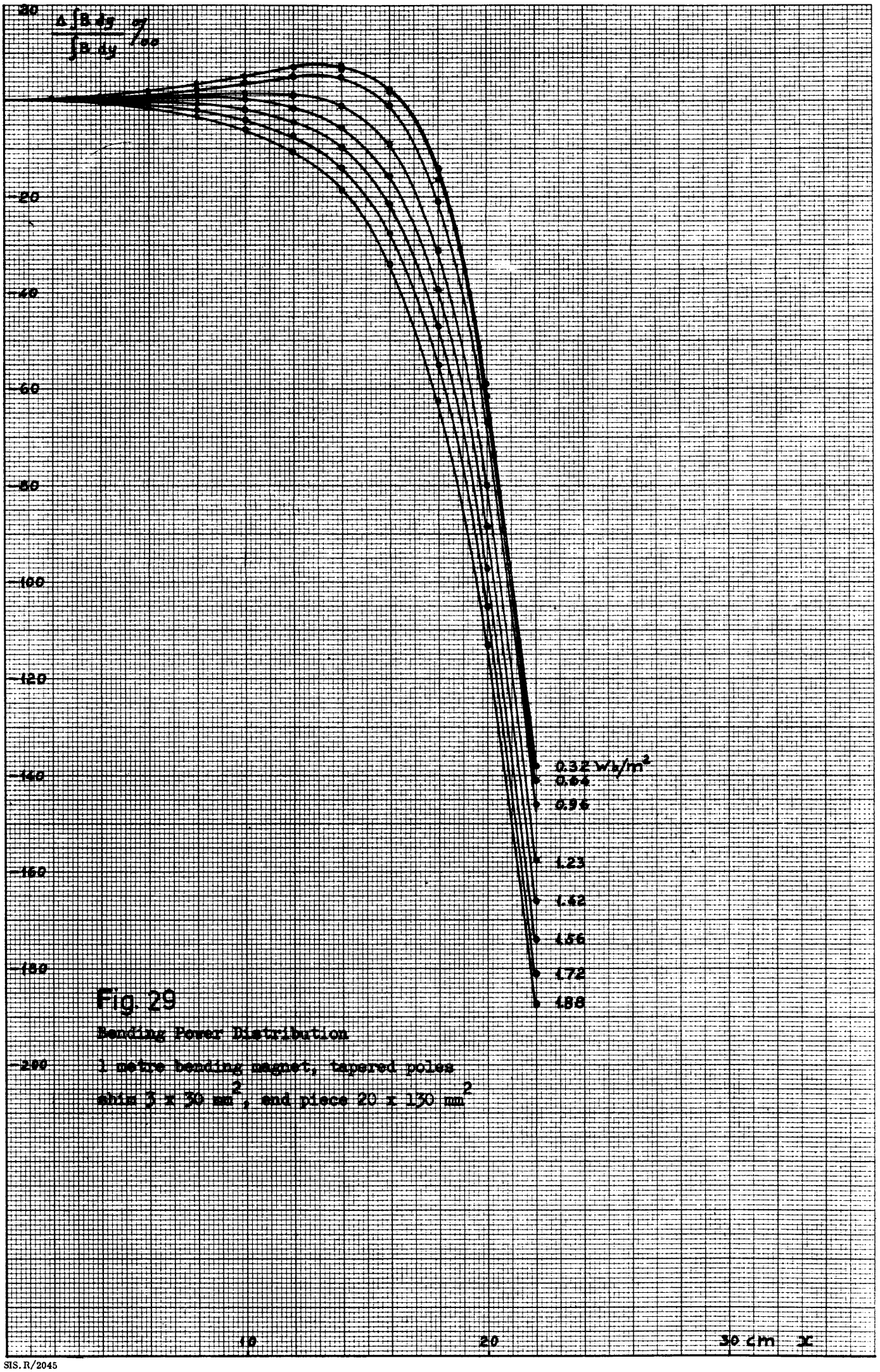

Fig. 29

Bending Power Distribution

1 metre bending magnet, tapered poles

shim 3 x 30 mm^2, end piece 20 x 130 mm^2

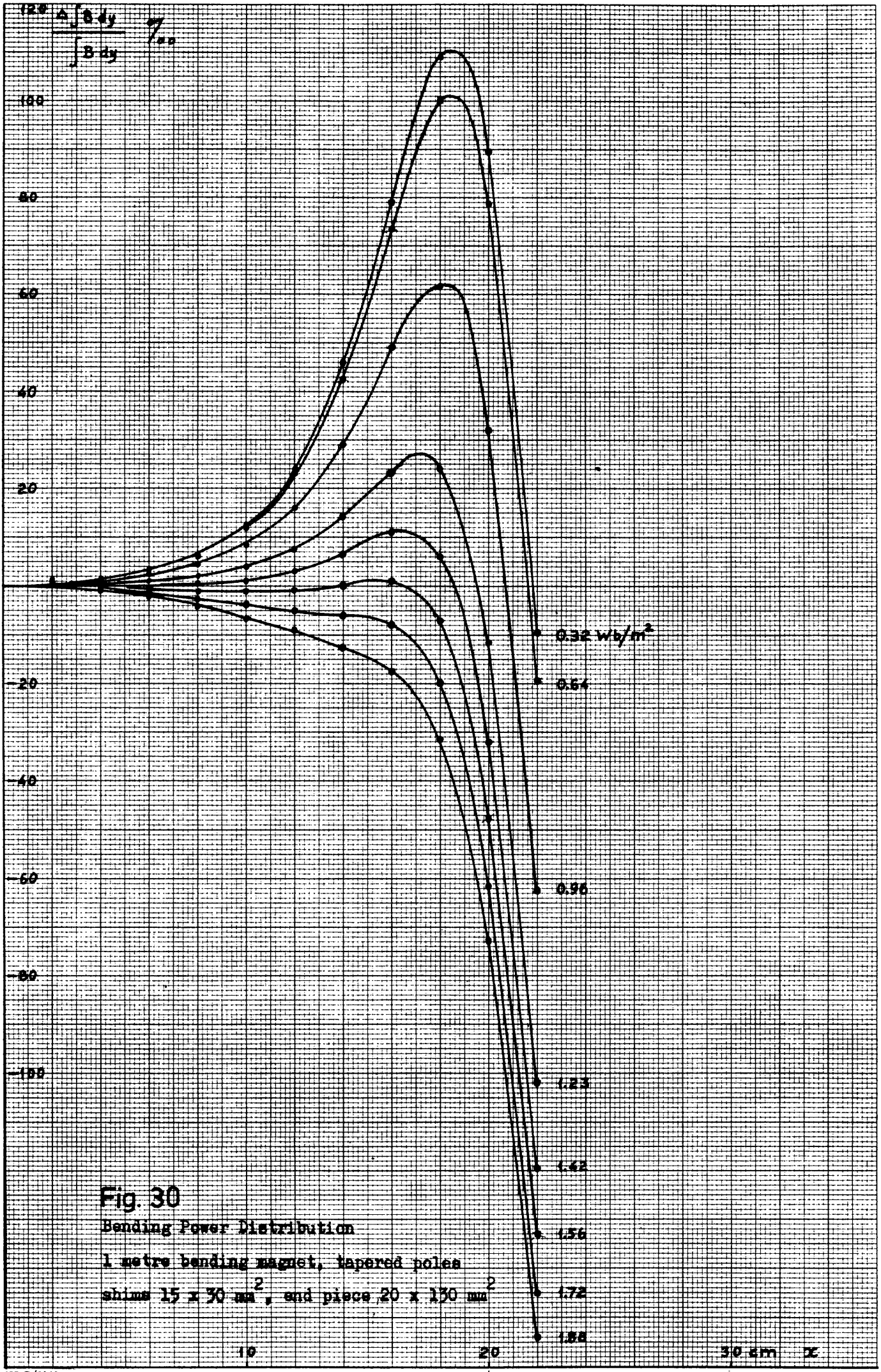

Fig. 30

Bending Power Distribution

1 metre bending magnet, tapered poles

shims 15 x 30 mm², end piece 20 x 130 mm²